AD-A158 895 THE EFFECT OF CONDENSATE INUNDATION ON STEAM CONDENSATION HEAT TRANSFER IN A TUBE BUNDLE(U) NAVAL POSTGRADUATE SCHOOL MONTEREY CA S K BROWER JUN 85 1/2

UNCLASSIFIED F/G 20/13 NL

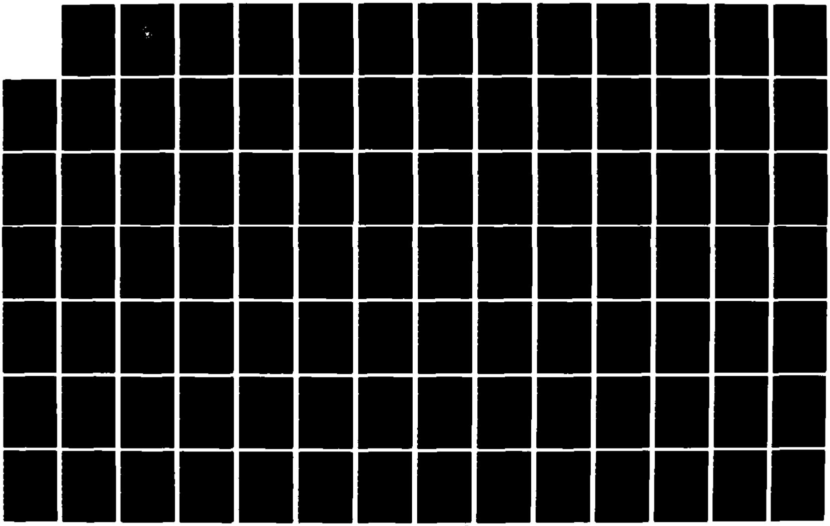

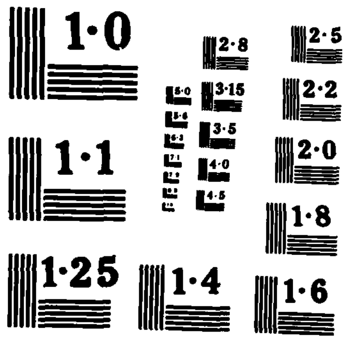
1·0
2·8
2·5
3·15
2·2
3·5
1·1
2·0
4·0
4·5
1·8
1·25
1·4
1·6

2

NAVAL POSTGRADUATE SCHOOL

Monterey, California

THESIS

THE EFFECT OF CONDENSATE INUNDATION ON STEAM CONDENSATION HEAT TRANSFER IN A TUBE BUNDLE

by

Steven K. Brower

June 1985

Thesis Co-Advisors: P.J. Marto
A.S. Wanniarachchi

REPORT DOCUMENTATION PAGE

READ INSTRUCTIONS BEFORE COMPLETING FORM

1. REPORT NUMBER	2. GOVT ACCESSION NO. AD A158 895
3. RECIPIENT'S CATALOG NUMBER	
4. TITLE (and Subtitle) The Effect of Condensate Inundation on Steam Condensation Heat Transfer in a Tube Bundle	5. TYPE OF REPORT & PERIOD COVERED Master's Thesis June 1985
	6. PERFORMING ORG. REPORT NUMBER
7. AUTHOR(s) Steven K. Brower	8. CONTRACT OR GRANT NUMBER(s)
9. PERFORMING ORGANIZATION NAME AND ADDRESS Naval Postgraduate School Monterey, California 93943-5100	10. PROGRAM ELEMENT, PROJECT, TASK AREA & WORK UNIT NUMBERS
11. CONTROLLING OFFICE NAME AND ADDRESS Naval Postgraduate School Monterey, California 93943-5100	12. REPORT DATE June 1985
	13. NUMBER OF PAGES 104
14. MONITORING AGENCY NAME & ADDRESS(if different from Controlling Office)	15. SECURITY CLASS. (of this report) Unclassified
	15a. DECLASSIFICATION/DOWNGRADING SCHEDULE

16. DISTRIBUTION STATEMENT (of this Report)

Approved for public release; distribution is unlimited

17. DISTRIBUTION STATEMENT (of the abstract entered in Block 20, if different from Report)

18. SUPPLEMENTARY NOTES

19. KEY WORDS (Continue on reverse side if necessary and identify by block number)

Steam condensation, heat-transfer coefficient, inundation, smooth, wire-wrapped tubes.

20. ABSTRACT (Continue on reverse side if necessary and identify by block number)

Steam-condensation heat-transfer measurements were made using a 5-tube in-line test condenser with an additional perforated tube to simulate up to 30 active tubes. Results were obtained for smooth tubes, wire-wrapped tubes and dropwise-coated tubes. The average outside heat-transfer coefficient for 30 smooth tubes was 0.64 times the Nusselt coefficient for the first tube. A total of eight wire-diameter and wire-pitch combinations were

#20 - ABSTRACT - (CONTINUED)

tested: 1.6-mm-diameter wire wrapped at 16 mm, 7.6 mm and 4 mm wire pitches, 1.0-mm-diameter wire wrapped at 8 mm, 4 mm and 2 mm wire pitches, and 0.5-mm-diameter wire wrapped at 4 mm and 2 mm wire pitches. The best bundle performance was obtained when the tubes were wrapped with 1.0-mm-diameter wire at a wire pitch of 4 mm. This combination resulted in an average outside heat-transfer coefficient for 30 tubes that was 1.15 times the value computed for the first tube using the Nusselt theory. The average outside heat-transfer coefficient for the 30 dropwise-coated tubes was 1.1 times the value of the heat-transfer coefficient for the first tube in the tube bundle. Utilizing either wire-wrapped tubes or dropwise-coated tubes, it is possible to significantly reduce the condenser surface area and overall size.

Approved for public release; distribution unlimited.

The Effect of Condensate Inundation on Steam Condensation Heat Transfer in a Tube Bundle

by

Steven K. Brower
Lieutenant, United States Navy
B.S., University of Idaho, 1975

Submitted in partial fulfillment of the requirements for the degree of

MASTER OF SCIENCE IN MECHANICAL ENGINEERING

from the

NAVAL POSTGRADUATE SCHOOL

June 1985

A1

Author: Steve Brower
Steven K. Brower

Approved by: P.J. Marto
P. J. Marto, Thesis Advisor

A. S. Wanniarachchi, Co-Advisor

P.J. Marto
P. J. Marto, Chairman,
Department of Mechanical Engineering

J N Dyer
John N. Dyer,
Dean of Science and Engineering

ABSTRACT

Steam-condensation heat-transfer measurements were made using a 5-tube in-line test condenser with an additional perforated tube to simulate up to 30 active tubes. Results were obtained for smooth tubes, wire-wrapped tubes and dropwise-coated tubes. The average outside heat-transfer coefficient for 30 smooth tubes was 0.64 times the Nusselt coefficient for the first tube. A total of eight wire-diameter and wire-pitch combinations were tested: 1.6-mm-diameter wire wrapped at 16 mm, 7.6 mm and 4 mm wire pitches, 1.0-mm-diameter wire wrapped at 8 mm, 4 mm and 2 mm wire pitches, and 0.5-mm-diameter wire wrapped at 4 mm and 2 mm wire pitches. The best bundle performance was obtained when the tubes were wrapped with 1.0-mm-diameter wire at a wire pitch of 4 mm. This combination resulted in an average outside heat-transfer coefficient for 30 tubes that was 1.15 times the value computed for the first tube using the Nusselt theory. The average outside heat-transfer coefficient for the 30 dropwise-coated tubes was 1.1 times the value of the heat-transfer coefficient for the first tube in the tube bundle. Utilizing either wire-wrapped tubes or dropwise-coated tubes, it is possible to significantly reduce the condenser surface area and overall size.

Inundation, Smooth [illegible]

TABLE OF CONTENTS

LIST OF TABLES

LIST OF FIGURES

NOMENCLATURE

A_o	Outside heat-transfer area of one tube (m^2)
A_F	Mean Vapor flow area (m^2)
A_i	Inside heat-transfer area of one tube (m^2)
B	Coefficient defined in equation (2.8)
C_f	Correction factor $(\mu_c/\mu_w)^{0.14}$
$C_{f,c}$	Calculated correction factor
C_i	Sieder-Tate coefficient
C_{pc}	Specific heat of water (kJ/kg·K)
D_F	Average flow dimension (m)
D_i	Inner diameter of the tube
D_o	Outer diameter of the tube
DT	Temperature difference (°C)
F	Dimensionless quantity defined in equation (2.8)
g	Acceleration of gravity (9.81 m/s^2)
h_{fg}	Latent heat of vaporization (kJ/kg)
h_i	Inside heat-transfer coefficient (W/m^2K)
h_N	Local, outside heat-transfer coefficient for the Nth tube (W/m^2K)
h_{Nu}	Heat-transfer coefficient calculated from the Nusselt equation (W/m^2K)
h_o	Outside heat-transfer coefficient (W/m^2K)
h_1	Outside heat-transfer coefficient for the first tube (W/m^2K)
k_c	Thermal conductivity of the cooling water (W/mK)
k_f	Thermal conductivity of the condensate film (W/mK)

k_m Thermal conductivity of Titanium (W/mK)

L Condensing length (m)

LMTD Logarithmic Mean Temperature Difference (K)

$\dot{m}_c$ Mass flow rate of cooling water (kg/s)

n Exponent defined in equation (2.8)

N The number of tubes in a column or the tube number of a given tube

Nu Water-side Nusselt number

P_L Longitudinal pitch of the tube bundle

P_r Prandtl number

P_T Transverse pitch of the tube bundle

q Heat flux based on the outside area (W/m^2)

Q Heat-transfer rate (W)

Re Water-side Reynolds number

$Re_{2\phi}$ Two-phase Reynolds number ($\rho_f V_v D_o / \mu_f$)

R_w Wall thermal resistance based on the outside area (m^2K/W)

s Inundation exponent defined in equation (5.1)

T_b Average cooling water bulk temperature (°C)

T_{ci} Cooling water inlet temperature (°C)

T_{co} Cooling water outlet temperature (°C)

T_{con} Condensate film temperature (°C)

T_f Average condensate film temperature (°C)

$T_{f,c}$ Calculated condensate film temperature (°C)

T_{sat} Saturation temperature of steam (°C)

T_{vap} Vapor temperature (°C)

T_w Wall temperature (°C)

U_o	Outside heat-transfer coefficient (m^2K/W)
V_c	Cooling water velocity (m/s)
V_v	Vapor velocity (m/s)
Y	Dimensionless quantity defined in equation (4.21)

GREEK SYMBOLS

μ_c	Dynamic viscosity of the cooling water ($N \cdot s/m^2$)
μ_f	Dynamic viscosity of the condensate film ($N \cdot s/m^2$)
μ_w	Dynamic viscosity of water ($N \cdot s/m^2$)
ρ_c	Density of the cooling water (kg/m^3)
ρ_f	Density of the condensate film (kg/m^3)
ρ_v	Density of the vapor (kg/m^3)

I. INTRODUCTION

A. HISTORICAL BACKGROUND

Considerable interest has been generated in reducing the size and the weight of propulsion systems for naval applications. Advances in condenser design could do much to reduce the size and the weight of the propulsion plant. Measures to raise the condensing-side heat-transfer coefficient (of condenser tubes) is one way to achieve this reduction in condenser size. This reduction, however, comes at a price. This is usually due to an increase in the pumping power or due to an increase in the initial cost of the tubes. For naval applications, where the size of a vessel may depend upon the size of the condenser (in a submarine, for example), this reduction in the size is justified, even at the greater cost.

Search [Ref. 1], at the Naval Postgraduate School, investigated the present condenser design process, and examined the potential benefits that might occur if heat-transfer enhancement was established in the condenser. He concluded that reductions of as much as forty percent in the size and weight of condensers are possible. This is dependent, of course, on the heat-transfer-enhancement technique utilized. Much further research work at the Naval Postgraduate School has been directed toward these heat-transfer-enhancement techniques.

Beck [Ref. 2], Pence [Ref. 3], Reilly [Ref. 4], Fenner [Ref. 5], and Ciftci [Ref. 6] conducted research employing a single-tube test condenser. Their research concluded that the overall heat-transfer coefficient of enhanced tubes may be as much as twice that for smooth tubes of similr geometry. In a separate report, Marto, Reilly and Fenner [Ref. 7] reported that most of the increase in the overall heat-transfer coefficient was on the cooling-water side and was due to an increase of the turbulence and the swirl, as well as to an increase in the inside surface area. Only a small increase occurred on the steam side.

Present-day steam condensers utilizing smooth tubes are limited in their thermal efficiency, due primarily to the large thermal resistances occurring on the tube side of the condenser. It is possible, however, by utilizing enhanced tubes, to increase the inside heat-transfer coefficient by 100 percent or more. The corresponding increase in the outside heat-transfer coefficient, however, is less than 50 percent. In studying ways to further increase the outside heat-transfer coefficient, Webb [Ref. 8] reported that conduction across the condensate film is the primary thermal resistance in film condensation. This thermal resistance is usually larger than the thermal resistance of the tube wall, that attributed to fouling or that due to noncondensable gases. It is possible to reduce this thermal resistance by utilizing a geometry that reduces the film thickness. This

reduction of the thermal resistance would mean a corresponding increase in the outside heat-transfer coefficient.

For large tube bundles, condensate inundation is present and must be considered when attempting to increase the overall heat-transfer coefficient. Thomas [Ref. 9] wrapped wire around smooth tubes in a helical manner and tested the condensation of ammonia in a large tube bundle. Increases of as much as 200 percent in the oustide heat-transfer coefficient over that predicted by Nusselt [Ref. 10] were measured. This increase was attributed to the effect of surface tension drawing the condensate to the wire and acting as a condensate run-off channel. In a paper by Cunningham [Ref. 11], "roped" tubes were considered and again the increase in the outside heat-transfer coefficient was attributed to condensate drainage, while an increase in the inside heat-transfer coefficient was attributed to the increase in the inside convective coefficient, due to the increased turbulence. Kanakis [Ref. 12] tested both smooth and roped tubes, with and without a wire wrap in an in-line tube bundle simulating up to 30 tubes. Adding the wire wrap on the smooth tube increased the average, outside heat-transfer coefficient for the 30 tube bundle by 50 percent, while adding the wire warp to the roped tube increased the average outside heat-transfer coefficient for the 30 tube bundle by more than 35 percent.

For condenser tubes, the increase in the outside heat-transfer coefficient may also be accomplished by promoting

dropwise condensation. Tanasawa [Ref. 13] reviewed dropwise condensation and discussed the methods for promoting these dropwise conditions. He concluded that the use of organic polymers (such as Teflon) was the most promising of all the dropwise-promoting techniques. Investigations of organic coatings by Brown [Ref. 14] have shown that enhancements of up to 180 percent are possible. Of primary concern, however, is that these coatings have very low conductivities and must therefore be ultra-thin. Another concern is that these coatings must be strongly adherent and sufficiently tough to withstand the conditions of their assembly and their use. Holden [Ref. 15] investigated numerous dropwise-promoting coatings. His tests were based not only on the ability of the coating to promote dropwise condensation, but also on the ability of the coating to sustain this dropwise performance over an extended period of time. In addition, the coatings that were able to sustain this dropwise performance were evaluated for their heat-transfer performance. His results indicated that the outside heat-transfer coefficient for a single tube could be increased by a factor of from five to eight through the use of polymer coatings.

Since the use of a wire wrap can increase the heat-transfer performance of a tube bundle, an important question arises: Is there some optimal wire diameter and wire pitch combination? In addition, during dropwise conditions what is the effect of condensate inundation upon heat transfer in a tube bundle?

B. OBJECTIVES

The objectives of this thesis were therefore to:

1. Conduct steam-condensation tests to determine the steam-side heat-transfer coefficient for 16-mm-o.d. smooth titanium tubes,

2. Confirm the heat-transfer-performance measurements of Kanakis [Ref. 12] on 16-mm-o.d. smooth titanium tubes with a 1.6-mm-o.d. titanium wire wrapped at a pitch of 7.6 mm,

3. Conduct heat-transfer-performance measurements to determine the effect of wire pitch and wire diameter on the steam-side heat-transfer coefficient with inundation, and

4. Conduct heat-transfer-performance measurements to determine the effect of inundation on a dropwise coated tube and compare this performance with the performance of a smooth tube.

II. THEORETICAL AND EMPIRICAL BACKGROUND

The basis for the analysis of film condensation on a horizontal tube was set forth by Nusselt in 1916. His analysis was, however, for laminar film condensation on a single horizontal tube. Nusselt's analysis yielded the well-known relationship for the heat-transfer coefficient:

$$h_{Nu} = 0.725\left[\frac{k_f^3\ \rho_f^2\ h_{fg}\ g}{D_o\ \mu_f(T_{sat}-T_w)}\right]^{1/4} \tag{2.1}$$

This relationship is subject to the following restrictions, as stated by Nobbs [Ref. 16]:

1. The wall temperature is constant,
2. The flow is laminar in the condensate film,
3. The film thickness is small compared to normal tube diameters,
4. All fluid properties are constant within the condensate film,
5. Heat transfer in the film is by conduction,
6. All forces due to hydrostatic pressure, surface tension, inertia, and vapor/liquid interfacial shear are negligible when compared to viscous and gravitational forces, and
7. The vapor/liquid interface and the surrounding steam are at the saturation temperature.

Jakob [Ref. 17] extended the Nusselt analysis to film condensation on a vertical in-line column of horizontal tubes by assuming that all the condensate from a tube drains

as a laminar sheet onto the tube below it. This is depicted in Figure 2.1a. In this idealized situation, the average coefficient for a vertical column of N tubes was predicted to be:

$$\overline{h_N} = 0.725\left[\frac{k_f^3\ \rho_f^2\ h_{fg}\ g}{D_o\ N\ \mu_f\ (T_{sat}-T_w)}\right]^{1/4} \qquad (2.2)$$

Combining equations (2.1) and (2.2) yields the Nusselt idealized theory for the average coefficient compared to the coefficient of the top tube:

$$\overline{h_N}/h_1 = N^{-1/4} \qquad (2.3)$$

In terms of the local heat-transfer coefficient for the Nth tube, this result becomes:

$$h_N/h_1 = N^{3/4} - (N-1)^{3/4} \qquad (2.4)$$

Realizing that condensate does not flow in a laminar sheet but by discrete droplets, Kern [Ref. 18] proposed a less-conservative relationship to account for the ripples and turbulence introduced into the condensate film. This is depicted in Figure 2.1b. The Kern relationship is:

$$\overline{h_N}/h_1 = N^{-1/6} \qquad (2.5)$$

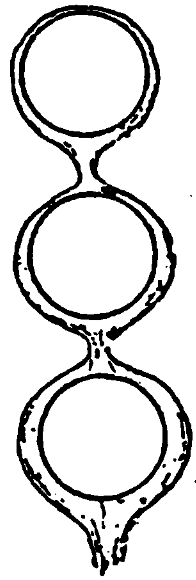

a. Nusselt's Idealized Laminar Flow Model

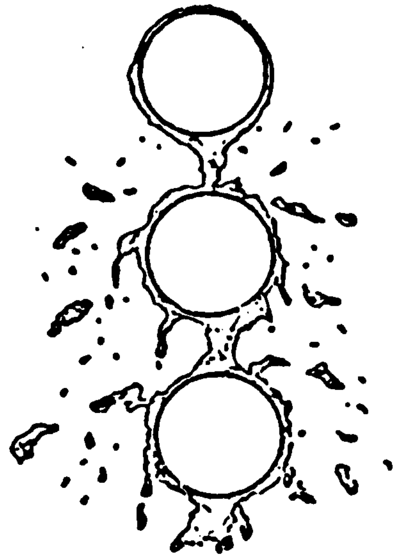

b. Kern's More Realistic Flow Model

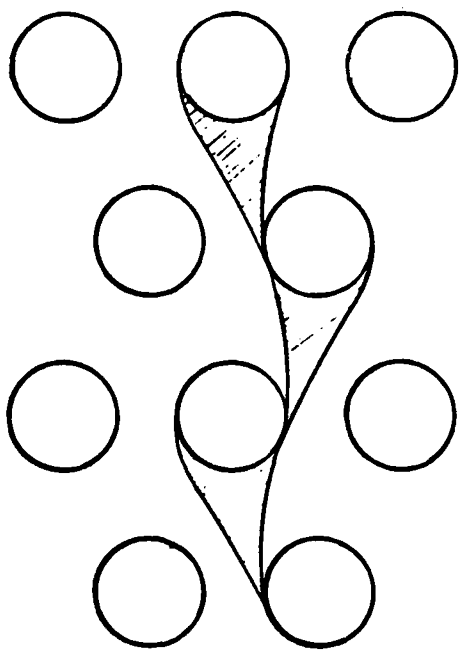

c. Eissenberg's Side-Drainage Flow Model

Figure 2.1 Representations of Condensate Flow

or in terms of the local heat-transfer coefficient for the Nth tube:

$$h_N/h_1 = N^{5/6} - (N-1)^{5/6} \tag{2.6}$$

Eissenberg [Ref. 19] did extensive experimentation to investigate the effects of steam velocity, condensate inundation and noncondensable gases on the condensation heat-transfer coefficient. He theorized that condensate does not always drain only onto tubes aligned vertically, but can be diverted sideways, especially in staggered tube bundles. The condensate draining sideways strikes the lower tubes on their sides rather than on their tops. This is depicted in Figure 2.1c. Since more heat is transferred from the top of a tube than from its bottom, the net effect of inundation is less severe. He predicted the following relationship:

$$\overline{h_N}/h_1 = 0.60 + 0.42\ N^{-1/4} \tag{2.7}$$

Extensive experimental research into the effect of condensate inundation has been conducted. However, the data exhibit a substantial amount of scatter as shown in Figure 2.2 by the cross-hatched area. Berman [Ref. 20] conducted a compilation of film condensation data on bundles of horizontal tubes and identified the following variables as important in causing the scatter:

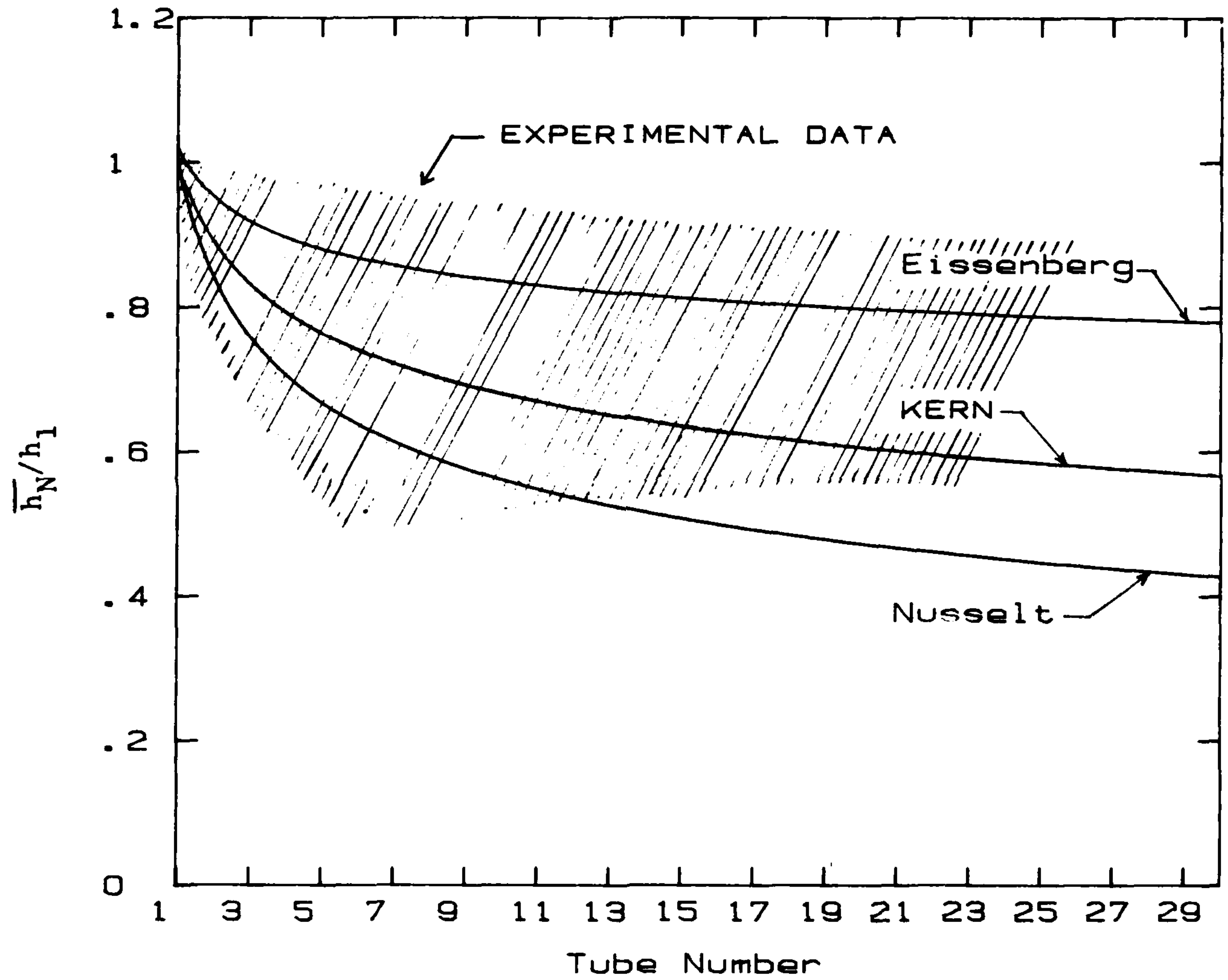

Figure 2.2 Theories and Data for Condensate Inundation

1. Bundle geometry (in-line or staggered),
2. Tube spacing,
3. Type of condensing fluid,
4. Operating pressure,
5. Heat flux, and
6. Local vapor velocity.

Marto and Wanniarachchi [Ref. 21] noted that other factors can have an effect on the data such as noncondensable gases, the direction of the vapor flow, partial dropwise conditions, an insufficient abount of steam reaching the lower tubes in the bundle and difficulty in the measurement of the local condensing coefficient.

Very small amounts of noncondensable gases can result in significant reductions in the condensation heat-transfer rate. Summaries of the phenomenon have been made by Chisholm [Ref. 22], and Webb and Wanniarchchi [Ref. 23]. The consensus among them is that noncondensable gases impose an added thermal resistance, since the vapor molecules must diffuse through a gas layer prior to reaching the condensing surface. These noncondensable gases can also lead to regions where the tubes are inoperative in a condensing role. Noncondensable gases have an adverse effect on the condenser performance, and must be taken into account when designing a tube bundle.

The motion of vapor within a condenser affects the film condensation process because of its effect on the surface

shear between the vapor and the film, and the resulting effect on vapor separation. Although the results may be different depending upon the orientation of the steam flow, the general effect of an increase in vapor velocity is a corresponding increase in the condensing heat-transfer coefficient. There exist a number of both theoretical and empirical equations representing vapor-shear effects on the condensate heat-transfer coefficient [Refs. 24, 25 and 26].

It is clear that the measurements that were made during this thesis had both inundation and vapor-shear effects. Marto [Ref. 27] stated that these two effects are difficult to separate from one another. During this study, however, an attempt was made to separate these two effects. For this purpose, data were taken on the top tube of the bundle with vapor velocity as a variable, and the data were correlated using an expression similar to a correlation suggested by Fujii [Ref. 28].

$$Nu/Re_{2\phi}^{1/2} = BF^n \qquad (2.8)$$

This correlation is based on numerous data for both staggered and in-line tube bundles. To represent the test-condenser tube bundle, the constants B and n in equation (2.8) were computed using a least-squares technique.

III. EXPERIMENTAL APPARATUS

The test facility was designed and built originally by Morrison [Ref. 29], and modified by Noftz [Ref. 30] and Kanakis [Ref. 12] to simulate an active tube column of up to 30 in-line tubes. A detailed description of all the components is contained in Ref. 30 and further modifications are described in Ref. 12. The descriptions in this report are brief, with particular focus given to the modifications undertaken by the author.

A. STEAM SUPPLY

The steam supply system is shown in Figure 3.1. House steam flows through a supply valve (MS-3), into a steam separator, and is throttled down by another valve (MS-4) to operating conditions. The steam then passes through an orifice and into the test condenser diffuser before entering the test condenser where it flows through a simulated in-line tube bundle.

B. TEST CONDENSER

The dimensions of the test condenser shown in Figure 3.2 were unchanged from Noftz's original design. The condenser consisted of five active tubes, twelve dummy tubes and one perforated tube. The tubes were positioned in the test condenser with a pitch-to-diameter ratio of 1.5. The active

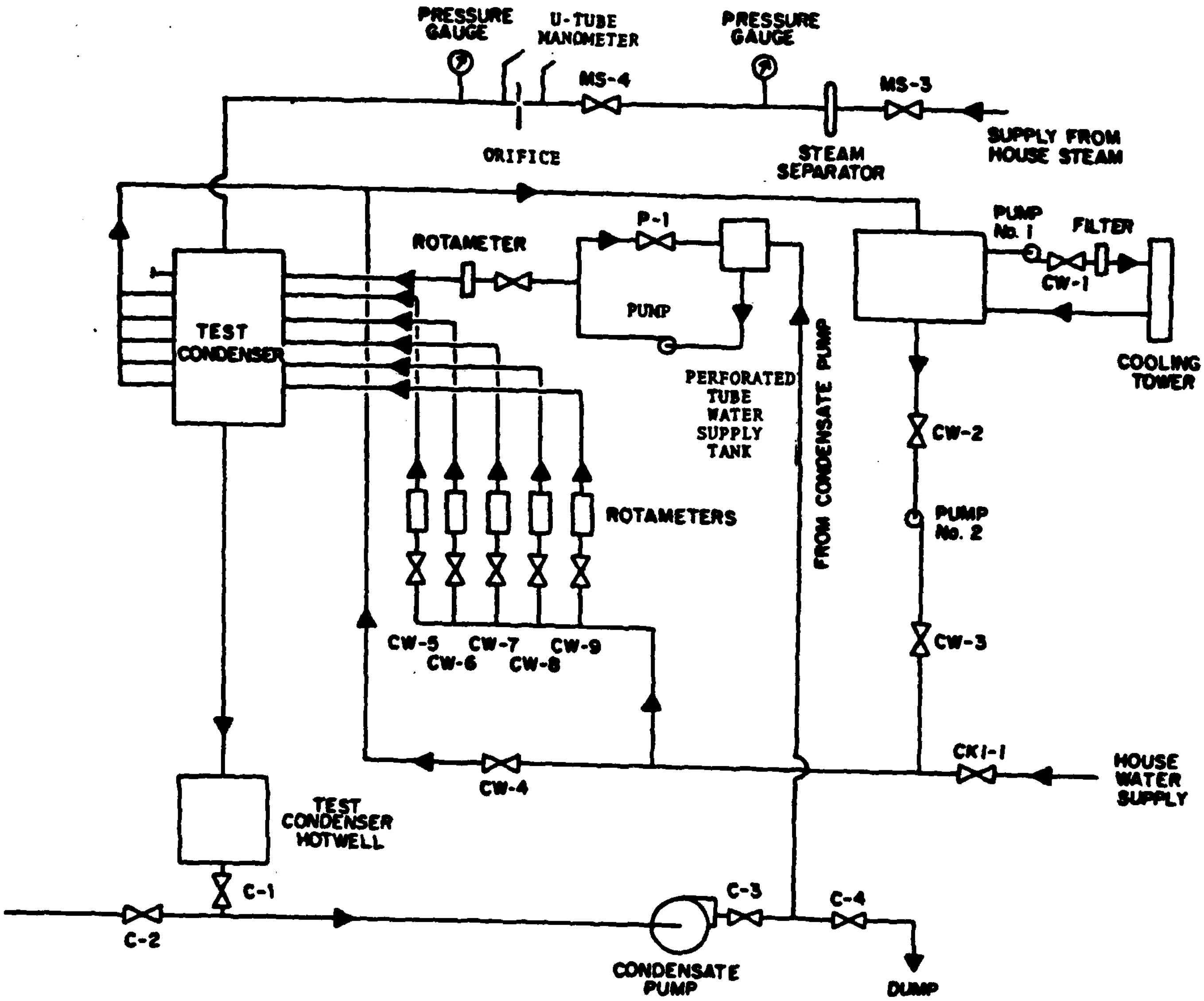

Figure 3.1 Schematic Diagram of Test Apparatus

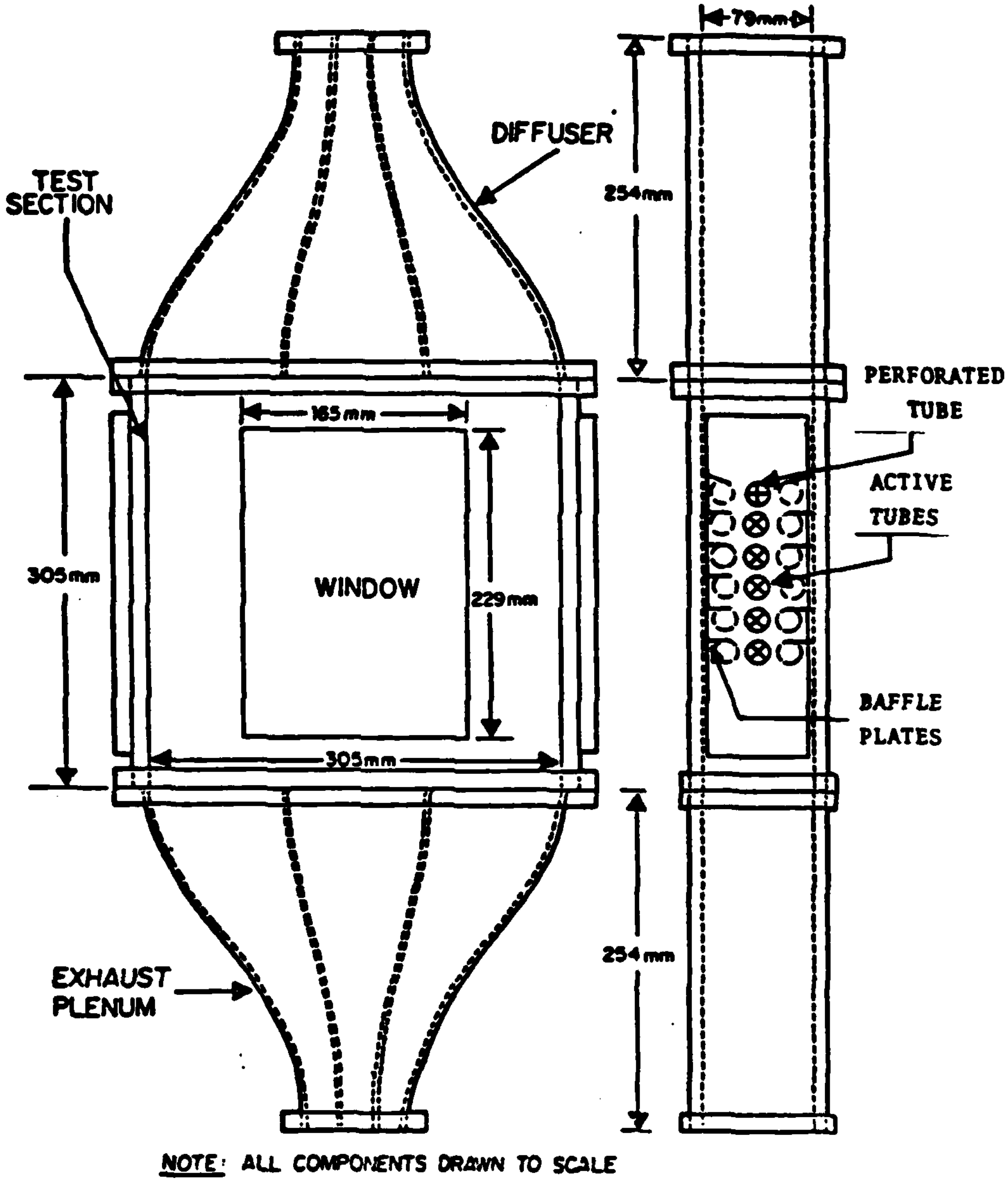

Figure 3.2 Sketch of Test Condenser

condensing length of each tube was 305 mm. A double-walled glass viewing window was provided on the front of the test condenser to allow for visual observation of the condensation process. Although the viewing window was designed to have heated air flowing between the glass walls, this feature was not utilized since no fogging of the glass was observed. A modification of the test condenser was made to minimize the steam flow along the test condenser side walls. The modification consisted of the addition of twelve baffle plates, placed as illustrated in Figure 3.2.

C. TEST-CONDENSER TUBES

Ten different types of active tubes were tested in this set of experiments. The tubes were manufactured by Wolverine Division of Universal Oil Products, and were made of titanium. All were of 16 mm o.d. and had a minimum wall thickness of 0.89 mm. The ten types of tubes are as listed below:

1. Smooth tubes,
2. Smooth tubes wrapped with 1.6-mm-o.d. titanium wire at three different pitches (16 mm, 7.6 mm and 4 mm),
3. Smooth tubes wrapped with 1.0-mm-o.d. titanium wire at three different pitches (8 mm, 6 mm and 4 mm),
4. Smooth tubes wrapped with 0.5-mm-o.d. titanium wire at two different pitches (4 mm and 2 mm), and
5. Smooth tubes with a dropwise coating.

The actual wrapping of the wire around the smooth tubes was performed by the author of this thesis. A detailed description of the procedure is included in Chapter III.

The dropwise-coated tubes were sent to General Magnaplate Corporation where a dropwise coating, commercially referred to as "Nedox," was applied. First an electro-deposited nickel-cobalt substrate was applied to the tube surface, and then this substrate was infused with a micro-thin Teflon layer. A heat-treating cycle was employed to ensure thorough infusion of the substrate with the Teflon. This coating is highly non-wetting, has a low coefficient of friction and is heat-resistant. The specifics of the "Nedox" process are proprietory, but the manufacturer claims control of the surface thickness to 0.0025 mm. For this thesis the requested surface thickness was 0.0075 mm.

D. PERFORATED TUBE

Each set of five active tubes had its own corresponding perforated tube. This perforated tube was located above the uppermost active tube; see Figure 3.2. Figure 3.3 shows a typical pattern for the perforations of a tube, and is an illustration of the supply-water tubing at the test condenser. This particular arrangement of the tubing was used in an attempt to provide an even flow from the entire length of the perforated tube. A heated tube was used to provide the water supply for the perforated tube. A separate rotameter was provided in order to control the rate of flow of condensate through the perforated tube.

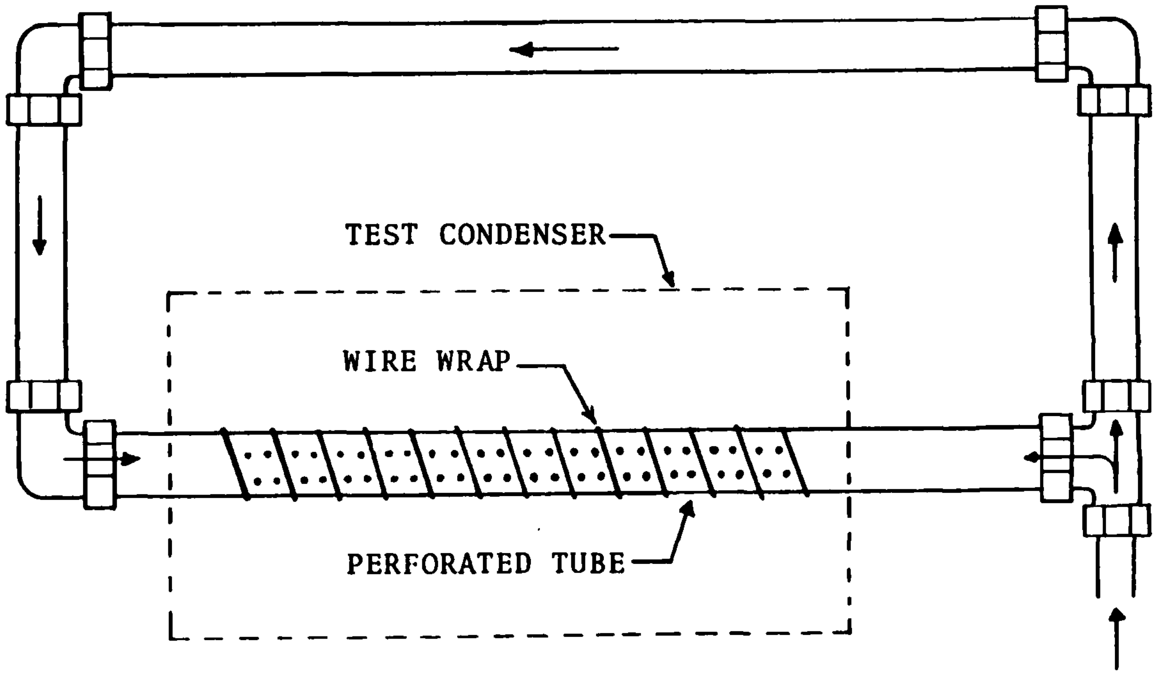

Perforated-tube water supply flow shown by arrows

Figure 3.3 Plan View of a Perforated Tube

E. CONDENSATE SYSTEM

The condensate system remained unchanged from Kanakis' modifications. Figure 3.1 shows the system as designed by Noftz and as modified by Kanakis. As steam condenses in the test condenser, it runs into and collects in the test condenser hotwell. The hotwell is a calibrated cylinder equipped with a sight glass, providing a visual measure of the condensate being produced. Measurement of the condensate collection rate provided the flow rate to be supplied to the perforated tube.

F. COOLING WATER SYSTEM

Although the cooling water system remained unchanged from Noftz original design, the five rotameters were recalibrated after Kanakis' data were taken. Each active tube had its own rotameter and regulating valve, and it was possible to control the coolant velocity through the active tubes up to values of 5 m/s. All data for this thesis, however, were taken at a constant coolant velocity of 1.56 m/s. The inlet temperature of the cooling water was maintained at a nearly constant temperature by the use of a large supply tank and a separate cooling tower to dissipate excess heat to the atmosphere. In order to provide a bulk temperature at the outlet of each active tube, a mixing chamber was installed just upstream of the temperature monitoring point.

G. INSTRUMENTATION

1. Flow Rates

Rotameters were used to measure the flow rate of the cooling water to each active tube and to the perforated tube.

2. Temperatures

Stainless-steel-sheathed copper-constantan thermocouples were used as the primary temperature monitoring devices. Table 1 lists the locations monitored by each of the thermocouples. Calibration, as performed by Kanakis, was utilized for all data taken.

The perforated-tube water supply was not maintainable at a constant temperature, nor was it quickly adjustable to a desired temperature. The system, as designed, contained a Gulton Industries, West 20 temperature controller. Although the manufacturer's accuracy was listed as 1.25 degrees F, the system response was so poor that the temperature of the perforated-tube supply water varied by as much as 10 degrees C from the beginning of the data run to the completion of the data run.

3. Pressure

A Bourdon-tube pressure gauge was used to measure the house steam supply pressure, while a compound pressure gauge was used to measure the steam pressure downstream of the orifice. A pressure transducer was used to measure the pressure in the test condenser, and a U-tube mercury manometer was fitted to measure the pressure drop across the orifice.

TABLE 1

Thermocouple Monitoring Locations

LOCATION	CHANNEL
T_{ci} #1	000
T_{ci} #3	001
T_{ci} #5	002
T_{co} #1	003
T_{co} #1	004
T_{co} #1	005
T_{co} #2	006
T_{co} #2	007
T_{co} #3	008
T_{co} #3	009
T_{co} #4	010
T_{co} #4	011
T_{co} #4	012
T_{co} #5	013
T_{co} #5	014
T_{sat}	015
T_{sat}	016
T_{con}	017
T_{vap}	018

4. Data Collection and Display

A Hewlett-Packard model 3054A Automatic, Data-Acquisition System, with a HP 2671G printer was used to record and display the thermocouple and transducer readings. The pressure transducer was assigned to channel 19 of the data-acquisition system, with the thermocouples assigned to the channels as indicated in Table 1.

IV. EXPERIMENTAL PROCEDURES

A. CALIBRATION

1. Rotameters

Calibration was performed on the five rotameters that supplied the cooling water to the active tubes. This calibration was performed using a weighing tank and a stop-watch, and a least-squares-fit calibration line was generated for each of the rotameters.

2. Steam Orifice

To calibrate the steam orifice the following steps were taken:

1. Set a steam flow rate,
2. Adjust the cooling water flow rate to condense all the incoming steam,
3. Measure the pressure drop across the orifice,
4. Measure the condensate collection rate,
5. Repeat steps 1 through 4 for different steam flow rates, and
6. Develop a least-squares-fit straight line for the steam mass flow rate vs. pressure drop.

B. PREPARATION OF CONDENSER TUBES

Prior to the winding of the titanium wire, the outside surface of the tubes was buffed using steel wool unitl all evidence of surface oxidation was removed. If any oxidation was evident on the inner surface of the tube, a test-tube

brush was used to apply a 50-percent sulfuric-acid solution to the inner surface of the tube. The tube was then thoroughly rinsed using tap water.

The procedure followed in the wrapping of the wire onto the smooth tubes was the same for every wire diameter and pitch combination tested. The wire was first welded to the tube and then, under a constant tension of 22 Newtons, the wire was guided (using a metal plate to control the spacing between the wire wraps) to the proper pitch as the tube was manually turned. Upon completion of the wrapping, the free end of the wire was then welded to the tube to yield a helically-wrapped surface 305 mm in length. After the wire wrapping of the tubes was completed and just prior to the installation of the tubes in the test condenser, the tubes were cleaned inside and out using a brush and a biodegradable detergent. A thorough rinsing was agin undertaken, and the tubes were checked to ensure that they displayed proper wetting characteristics. If any non-wetting areas were evident, a 50-percent solution of sodium hydroxide mixed with an equal amount of ethyl alcohol and heated to about 80 degrees C, was brushed onto the tube surface. After rinsing with tap water, the tube was ready for installation in the test condenser. Upon completion of the installation of the tubes in the test condenser, steam was introduced into the test condenser. Again the tubes were visually examined. If there were any areas that displayed dropwise condensation, the tubes were

washed from above using the perforated-tube water supply. This was sufficient in all cases to restore filmwise condensation.

C. SYSTEM OPERATION

The system was operated in accordance with the operating instructions outlined in Appendix A of Ref. 17. The system was deemed to be operating at a steady-state condition when the cooling water inlet temperature was steady. The cooling water inlet temperature was monitored using the HP-3054A Automatic Data Acquisition System, and was considered steady when two consecutive readings (at five-minute intervals) varied by less than 0.1 degrees C.

One hour was usually required from system start-up to the steady-state condition. Upon reaching the steady-state condition, a data run was begun. Any changes in the cooling water flow or changes in the perforated-tube water flow were accompanied by a five-minute wait for system restabilization, prior to taking any further data. The duration of each data set was approximately one minute, and a completed data run consisted of 30 separate data sets. During each data set, the condensation collection rate was measured. For each inundation condition, five consecutive data sets were taken and the average values were computed. After each set of five consecutive data sets, the average condensate collection rate was used to determine the rate of flow of the water into the perforated tube which was to be used for the next set of

data (the average amount of condensate collected during a data set was introduced into the perforated tube for the next inundation condition). For example, to simulate tubes 6 through 10, the perforated-tube water flow rate was set equal to the condensate collection rate for tubes 1 through 5. A data run was considered completed upon the simulation of inundation conditions through the 30th tube.

Thermocouple readings and pressure-transducer readings were taken automatically by the data-acquisition system, while the settings of the rotameters and the test condenser initial and final hotwell levels were entered into the computer using the keyboard. Initial and final hotwell levels were taken for a time interval of one minute.

The following conditions were the operating conditions for all data taken for this thesis:

1. The coolant velocity was 1.55 ± 0.05 m/s,
2. The coolant inlet temperature was 24 degrees C. (± 3 degrees C. depending on the day of the run, but constant during a given run), and
3. The saturation temperature was 100.5 ± 0.5 degrees C.

D. DATA-REDUCTION PROGRAM

A computer program was utilized to process and plot all raw data. The program was written in BASIC language and was run on an HP-9826 computer. A listing of this program is included as Appendix C.

E. HEAT-TRANSFER-COEFFICIENT CALCULATION

1. Inside Heat-Transfer Coefficient

The inside heat-transfer coefficient was computed using the Sieder-Tate equation described in Holman [Ref. 31]:

$$Nu = h_i D_i / k_c = C_i Re^{0.8} Pr^{1/3} (\mu_c/\mu_w)^{0.14} \tag{4.1}$$

where the coefficient C_i was computed using a modified Wilson plot [Ref. 12]. Using this technique, Kanakis [Ref. 12] obtained a Sieder-Tate coefficient of 0.029 ± 0.001. The method Kanakis used, however, did not include the variation of the condensate film properties as a function of heat flux. A slightly different, modified Wilson plot, as described by Nobbs [Ref. 16], that does account for this variation in the film properties, was used in this thesis. Appendix D gives a description of this method. Reprocessing Kanakis' data with this method, the Sieder-Tate coefficient was determined to be 0.028 ± 0.001.

2. Outside Heat-Transfer Coefficient

The heat-transfer rate to the cooling water can be computed using an energy balance, and can be expressed in terms of an overall heat-transfer coefficient by:

$$Q = \dot{m}_c c_{pc} (T_{co} - T_{ci}) = U_o A_o \, LMTD \tag{4.2}$$

where

$$\mathrm{LMTD} = \frac{T_{co} - T_{ci}}{\ln((T_{sat} - T_{ci})/(T_{sat} - T_{co}))} \qquad (4.2a)$$

Solving for the overall heat-transfer coefficient gives:

$$U_o = \dot{m}_c \, c_{pc}/A_o \, \ln((T_{sat} - T_{ci})/(T_{sat} - T_{co})) \qquad (4.3)$$

The overall thermal resistance can be written as the sum of the internal, wall and external resistances:

$$\frac{1}{U_o \, A_o} = \frac{1}{h_i \, A_i} + \frac{R_w}{A_o} + \frac{1}{h_o \, A_o} \qquad (4.4)$$

where

$$R_w = D_o \ln(D_o/D_i)/2 \, k_m \qquad (4.4a)$$

or from this result, the outside heat-transfer coefficient may be written:

$$h_o = \frac{1}{1/U_o - D_o/D_i \, h_i - R_w} \qquad (4.4b)$$

F. DATA-REDUCTION TECHNIQUE FOR THE OUTSIDE HEAT-TRANSFER COEFFICIENT

A listing of the computer program used in the calculation of the outside heat-transfer coefficient can be found in Appendix C. The steps required in the technique are outlined below:

1. Calculate the average bulk cooling water temperature:

$$T_b = (T_{co} + T_{ci})/2 \tag{4.5}$$

2. Calculate the cooling water velocity:

$$V_c = \dot{m}_c/A_i \, \rho_c \tag{4.6}$$

3. Calculate the cooling water Reynolds number:

$$Re = \rho_c \, V_c \, D_i/\mu_c \tag{4.7}$$

4. Calculate the heat transferred to the cooling water using the left-hand side of equation (4.2).

5. Calculate the heat flux:

$$q = Q/(\pi \, D_o \, L) \tag{4.8}$$

6. Since the film temperature was not a known quantity, an iterative scheme was employed to calcualte the film temperature, as indicated below:

   a) Assume a film temperature (say $T_f = T_{sat}$),

   b) Calculate the Nusselt coefficient,

$$h_{Nu} = 0.651 \left[\frac{k_f^3 \, \rho_f^2 \, h_{fg} \, g}{\mu_f \, D_o \, q} \right]^{1/3} \tag{4.9}$$

   c) Evaluate $T_{f,c}$, and

$$T_{f,c} = T_{sat} - \frac{q}{2 \, h_{Nu}} \tag{4.10}$$

d) Repeat steps a) through c) until $T_{f,c}$ is approximately equal to T_f.

7. Calculate the inside heat-transfer coefficient:

$$h_i = k_c C_i Re^{0.8} Pr^{1/3} C_f/D_i \tag{4.11}$$

where C_f is the correction factor $(\mu_c/\mu_w)^{0.14}$. (4.11a)

8. Since the correction factor is evaluated at the inner wall temperature, an iterative scheme was employed to calculate the wall temperature as indicated below:

a) Assume a value for C_f (e.g., 1.0),

b) Calculate h_i using equation (4.11),

c) Calculate a water-side temperature drop,

$$DT = q D_i/h_i D_o \tag{4.12}$$

d) Calculate a new correction factor, and

$$C_{f,c} = (\mu_c/\mu_w)^{0.14} \tag{4.13}$$

e) Repeat steps a) through d) until $C_{f,c}$ is approximately equal to C_f.

9. Calculate the log-mean-temperature difference using equation (4.2a).

10. Calculate the overall heat-transfer coefficient:

$$U_o = q/LMTD \tag{4.14}$$

11. Calculate the outside heat-transfer coefficient using equation (4.4b).

12. Calculate the normalized, local, outside heat-transfer coefficient.

$$h_N/h_1$$

13. Calculate the normalized, average, outside heat-transfer coefficient.

$$\overline{h_N}/h_1$$

NOTE: In the above formulation, the thermal resistances due to noncondensable gases and any fouling were assumed to be negligible.

G. DATA-REDUCTION TECHNIQUE FOR THE VAPOR-SHEAR CORRELATION

For the calculation of the vapor-shear correlation, measurements on only the first active tube in the tube bundle were taken.

1. Calculate the inside heat-transfer coefficient as outlined above.

2. Calculate the outside heat-transfer coefficient as outlined above.

3. Calculate a temperature correction:

$$DT = q/h_o \tag{4.15}$$

4. Assume a film temperature:

$$T_f = T_{sat} - DT/2 \tag{4.16}$$

5. Calculate the steam velocity:

$$V_v = m_v \, v_v / A_f \tag{4.17}$$

where

$$A_F = 2 \, L(P_T \, P_L - \pi \, D_o^2/4)/P_L \tag{4.17a}$$

A_F is the Mean Vapor Flow Area defined by Nobbs [Ref. 16] and depicted in Figure 4.1.

6. Calculate the two-phase Reynolds number:

$$Re_{2\phi} = \rho_f \, V_v \, D_o / \mu_f \tag{4.18}$$

7. Calculate the dimensionless quantity F:

$$F = D_o \, \mu_f \, h_{fg} \, g / V_v^2 \, k_f \, DT \tag{4.19}$$

8. Calculate the Nusselt number:

$$Nu = h_o \, D_o / k_f \tag{4.20}$$

9. Calculate Y:

$$Y = Nu/Re_{2\phi}^{1/2} \tag{4.21}$$

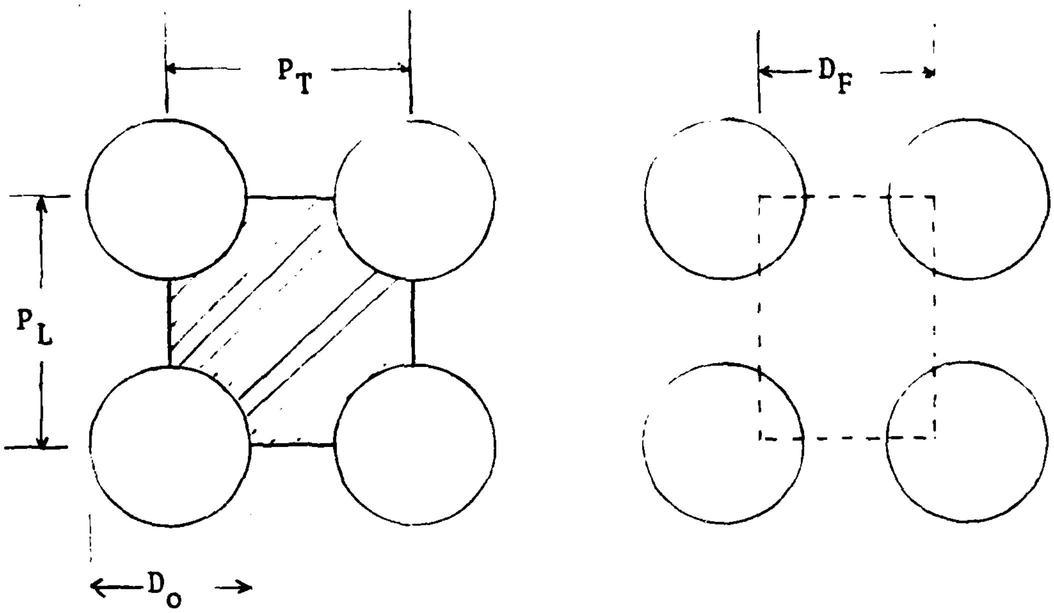

To calculate the mean flow area the following steps are required:

1) Calculate the cross-hatched area above,

   AREA = $P_T \, P_L - \pi \, D_o^{\,2} / 4$

2) Divide by longitudinal pitch to obtain an average flow dimension

   D_F = AREA / P_L

3) Multiply by the condenser length and the number of flow paths (2 flow paths in the case of this thesis).

   $A_F = 2 \, L \, (P_T \, P_L - \pi \, D_o^{\,2} / 4) / P_L$

Figure 4.1 Mean Vapor Flow Area

10. Repeat steps 1 through 9 at different steam mass flow rates into the test condenser. For this thesis 10 different steam mass flow rates were considered, and three measurements taken at each mass flow rate.

11. Starting with an assumption that the data would be of a form similar to that postulated by Fujii [Ref. 28], an expression was assumed:

$$Y = B\,F^{n}; \text{ F as defined in equation (4.19)} \qquad (4.22)$$

12. Perform a least-squares-fit of the data and determine the constant B and the exponent n.

V. RESULTS AND DISCUSSION

A. RESULTS BEFORE AND AFTER TEST CONDENSER MODIFICATION

Initially, data were taken with the test condenser used by Kanakis [Ref. 12], with no modifications. As can be seen from Figure 5.1, the nondimensionalized heat-transfer coefficient exhibits a saw-toothed variation over the inundation range considered. The particular wire pitch and wire diameter combination chosen for Figure 5.1 was representative of the pattern apparent in the data sets taken prior to the test-condenser modification.

It was determined that the original design of the test condenser allowed too much steam to bypass the five active tubes, thereby allowing the steam to flow between the walls of the test condenser and the two rows of dummy tubes. Since steam was bypassing the active tubes, inadequate steam was flowing in the vicinity of the active tubes. This led to artificially low heat-transfer readings in the lower tubes of the tube bundle. To minimize this problem, baffle plates were installed on each side of the test condenser as described previously (Figure 3.2).

After the placement of the baffle plates, the previously tested tube sets were retested. As can be seen in Figure 5.1, the saw-toothed variation of the curve is much less pronounced and appears to be nearly corrected. The net effect of the removal of the saw-toothed variation by the

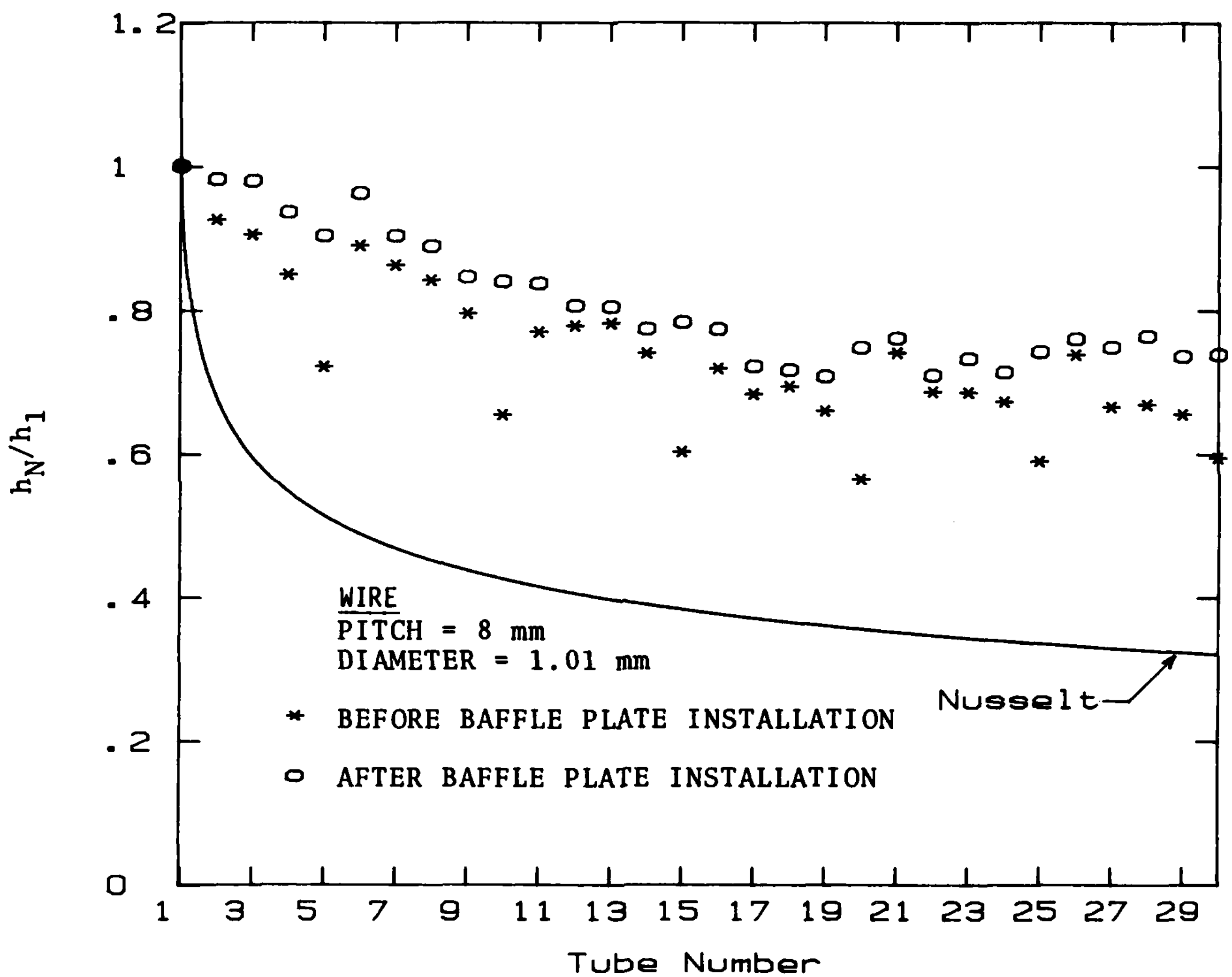

Figure 5.1 Data With and Without Baffles

installation of the baffle plates is an increase in the measured heat-transfer coefficient. This, in turn, means that the effect of inundation is not actually as great as had been earlier suspected. All data represented in this report will, hereafter, be with the baffles in place.

B. VAPOR-SHEAR CORRELATION

As discussed previously, the vapor shear correlation was assumed to be of the form postulated by Fujii [Ref. 28]--see equation (4.8). Figure 5.2 is the graph of Y vs. F for the first active smooth titanium tube. For this tube, the value of B was determined to be 0.834 and the value of n was determined to be 0.166. These results fall about 15 percent below the Fujii correlation [Ref. 28] ($B = 0.96$ and $n = 0.20$). There are several possible explanations for this difference.

1. Both the value of Y and the value of F are partly based on the steam velocity, with a higher value of steam velocity resulting in a lower value for both Y and F. During this thesis, the steam velocity was only varied from 1.4 to 2.1 m/s. The corresponding range of F was therefore from 3.6 to 1.5, while the corresponding range of Y was from 1.1 to 0.8. Since the range of both F and Y were considerably more extensive for the calculation of the Fujii correlation, this is a possible explanation for the discrepancy.

2. For the Fujii correlation, both in-line and staggered tube bundles were considered. This could also be a possible reason for the discrepancy.

3. The direction of the steam flow considered for the determination of the Fujii correlation included vertically downward flow, vertically upward flow and also horizontal flow. This difference in flow directions is another possible explanation for the discrepancy between the correlation determined in this report and the Fujii correlation.

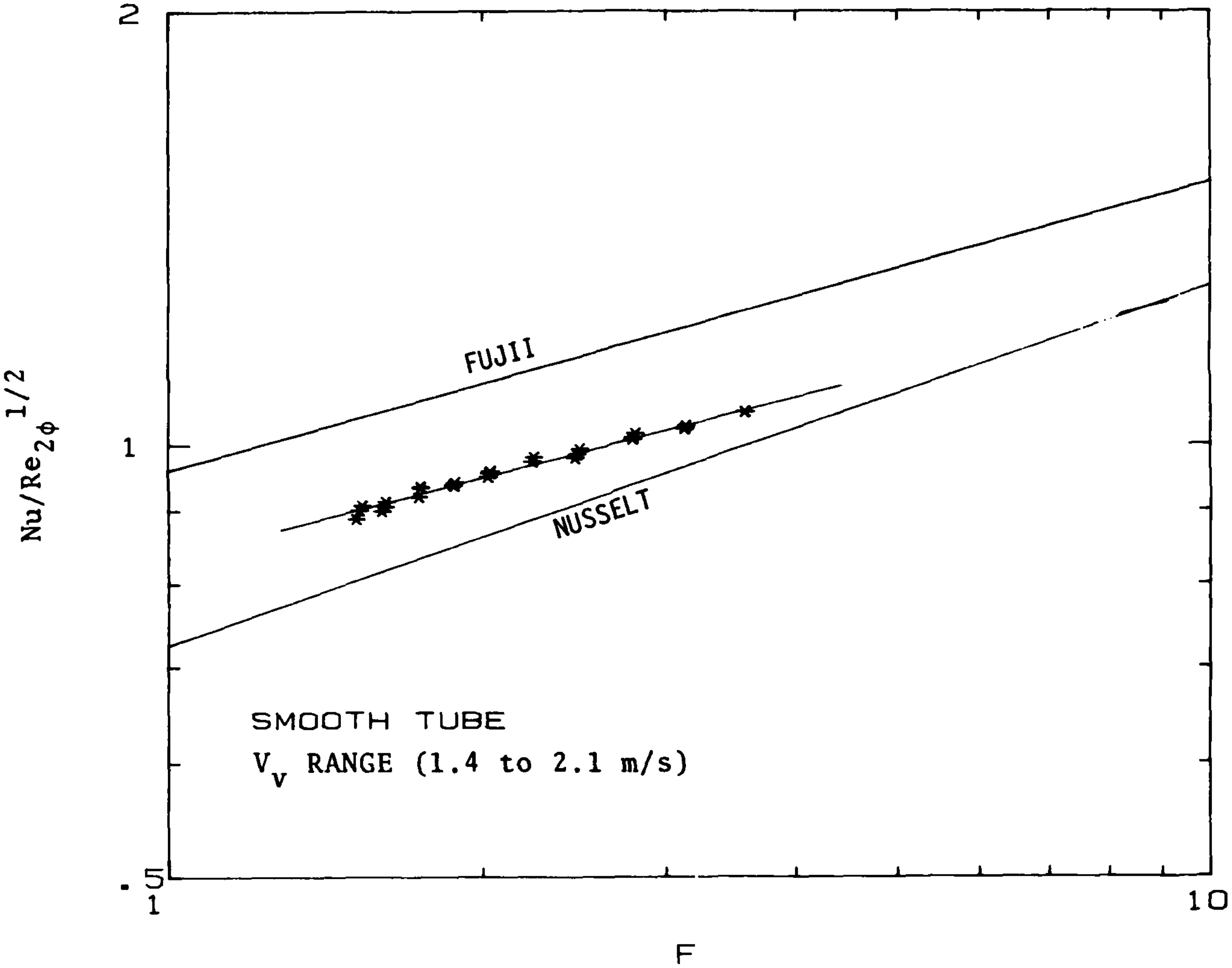

Figure 5.2 Vapor-Shear Correlation

4. As mentioned previously, baffle plates were installed in order to reduce the steam bypassing the active tubes. Even though the baffles reduced the amount of steam bypassing the active tubes, this is no guarantee that the steam still able to bypass the active tubes could not have had some influence on the vapor-shear correlation calculated in this thesis.

Since Reference 28 does not specifically say how the flow area used in his correlation was determined, this is another possible area for discrepancy. In addition, Fujii [Ref. 28] does not show which tube in the bundle was used for the formulation of his correlation. The actual location would have an important effect on the vapor velocity and could be another possible area for discrepancies to develop.

Vapor-shear correlations were determined for all of the tube sets tested for this report. Table 2 is a summary of the constants determined for the vapor-shear correlations.

C. THE EFFECT OF INUNDATION ON A SMOOTH TUBE BUNDLE

1. With Vapor-Shear Contribution Present

Figure 5.3 shows the variation of the normalized, local heat-transfer coefficient for up to 30 tubes. The value for the normalized, local heat-transfer coefficient for the 30th tube is approximately 45% above the value predicted by Nusselt theory, but very near the value predicted by the Kern relationship. As discussed in Chapter II, the Nusselt theory for a tube bundle is based on idealized laminar flow from tubes above to tubes below. The idealizations of Nusselt result in a conservative estimate of the heat-transfer coefficient, so the fact that the data are 45% above the

TABLE 2

Vapor-Shear Correlations

TUBE SET	WIRE DIAMETER (mm)	PITCH (mm)	B	n
1	Smooth tube		0.834	0.185
2a	1.58	16	0.835	0.178
b	1.58	7.6	0.837	0.189
c	1.58	4	0.725	0.192
3a	1.01	8	0.916	0.161
b	1.01	6	0.871	0.173
c	1.01	4	0.876	0.220
4a	0.50	4	1.036	0.200
b	0.50	2	0.915	0.192
5	Dropwise-coated tube		0.796	0.166

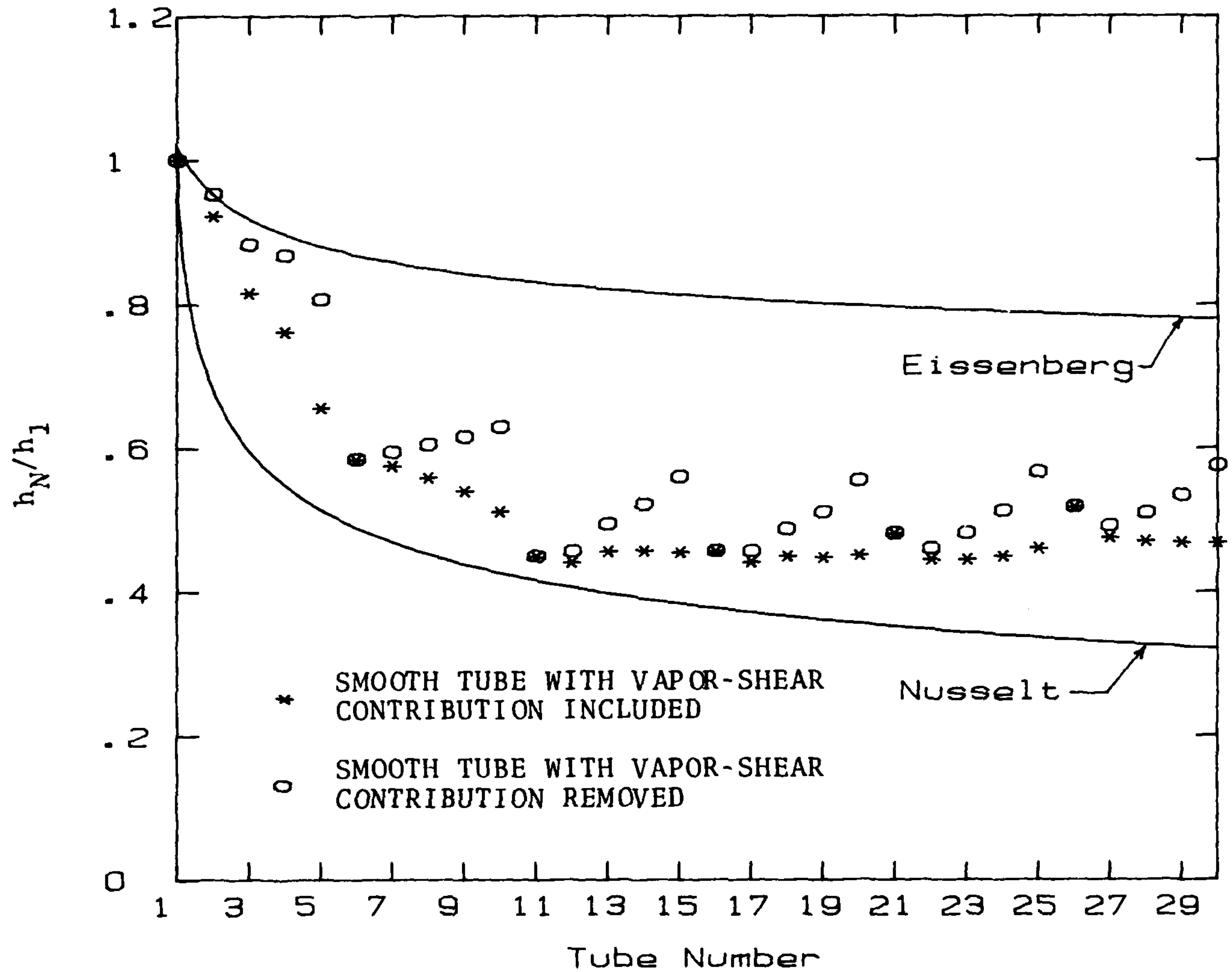

Figure 5.3 Inundation Effect on a Smooth Tube Bundle (Normalized, Local Heat-Transfer Coefficient)

Nusselt prediction is not totally unexpected. Since the Kern relationship is a more realistic view of the condensate action in the tube bundle, one would expect the data to be much nearer to the Kern relationship--as it is. The close agreement with the Kern relationship also was considered to be an indication that the test apparatus were operating properly.

Figure 5.4 shows the normalized, average heat-transfer coefficient for up to 30 tubes. The curve generated by these data is much smoother than the curve generated by the normalized, local heat-transfer coefficients. The value for the normalized, average heat-transfer coefficient of the 40th tube lies about 26% above the value predicted by Nusselt, but lies only 5% below the value predicted by Kern. Assuming a generalized form of the average heat-transfer coefficient for N tubes, divided by the heat-transfer coefficient for the first tube in the bundle, yields:

$$\overline{h_N}/h_1 = N^{-s} \qquad (5.1)$$

Referring to Figure 5.4, the dashed line roughly following the data represents a least-squares-fit exponential curve for the data, and the exponent derived is s = 0.183. This exponent and the exponent suggested by Kern (s = 0.167) are in reasonable agreement.

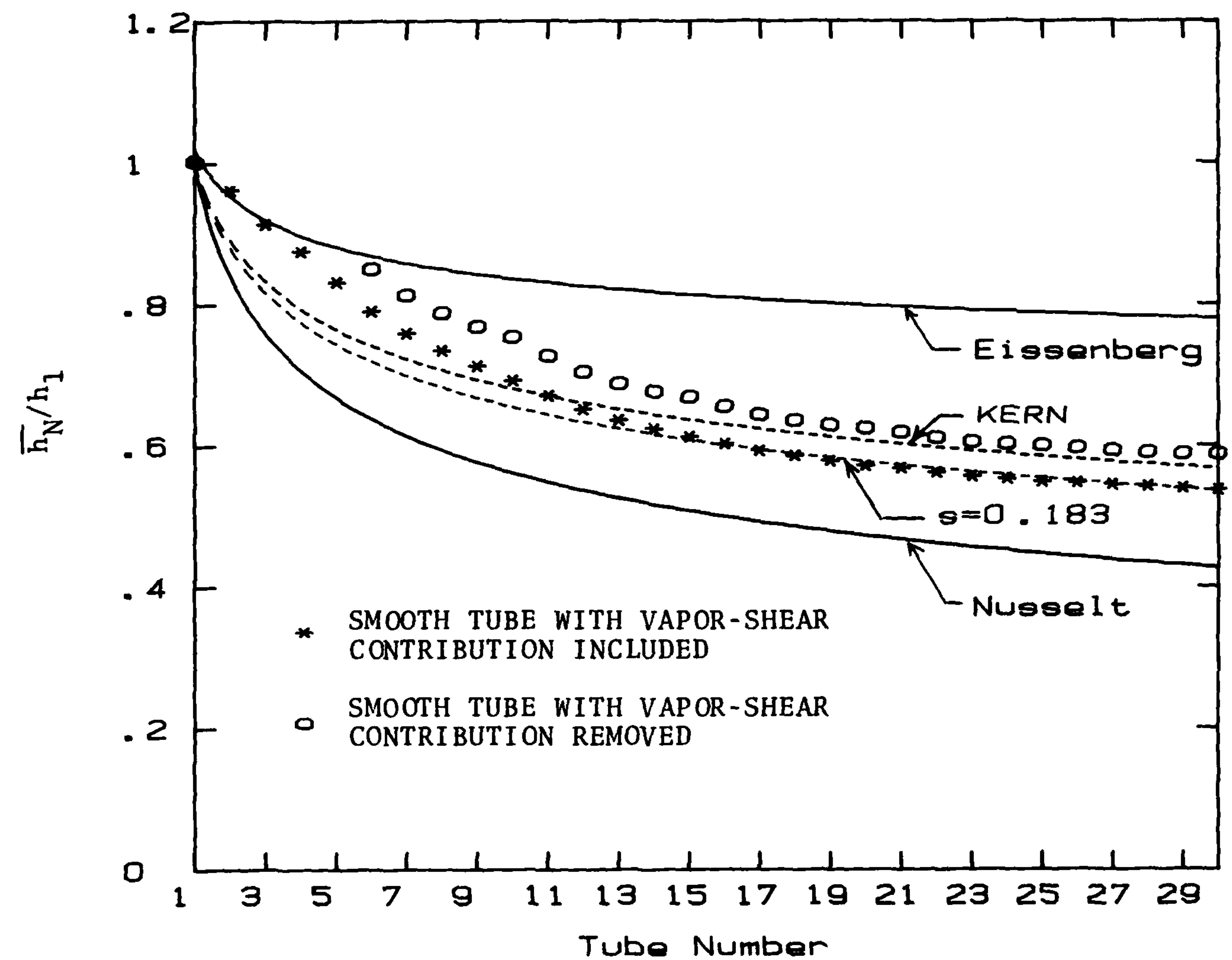

Figure 5.4 Inundation Effect on a Smooth Tube Bundle (Normalized, Average Heat-Transfer Coefficient)

2. With Vapor-Shear Contribution Removed

Figure 5.3 shows the variation of the normalized, local heat-transfer coefficient for up to 30 tubes with the contribution due to vapor shear removed. The vapor-shear correlation used was the one presented earlier in this report (B = 0.834 and n = 0.185). As can be seen from the graph, the trend in the data has now become a reversed saw-tooth. This is an indication of overcorrecting for the effect of vapor shear. This unacceptable trend in the data shows that mathematical separation of the vapor-shear contribution is not possible as stated by Marto [Ref. 27]. Therefore, throughout the remainder of this thesis the vapor-shear contribution is included, and no further attempt is made to remove the contribution due to vapor shear.

D. THE EFFECT OF INUNDATION ON SMOOTH TUBES WRAPPED WITH 1.6-MM-O.D. WIRE

Even though three different pitches (16 mm, 7.6 mm and 4 mm) were tested at this wire diameter, only the graph for the optimum pitch will be presented for the normalized, local heat-transfer coefficient for a bundle of up to 30 tubes. The graph for the pitch of 7.6 mm is presented in Figure 5.5. The value for the normalized, local heat-transfer coefficient for the 30th tube is approximately 170% above the value predicted by the Nusselt theory and approximately 83% above the value predicted by the Kern relationship.

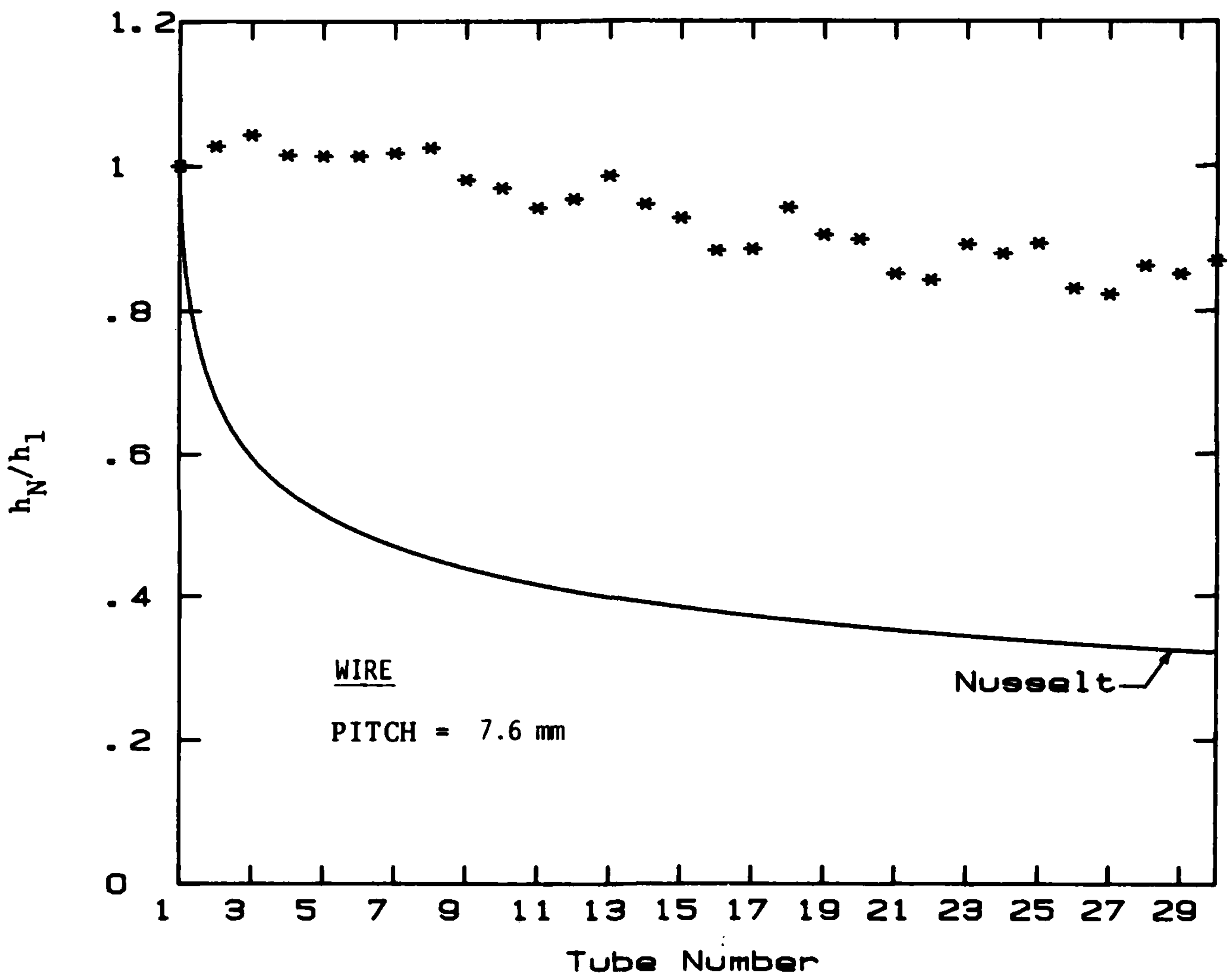

Figure 5.5 Effect of 1.6-mm-o.d. Wire on Inundation (Normalized, Local Heat-Transfer Coefficient)

Figure 5.6 shows the normalized, average heat-transfer coefficient for a bundle of up to 30 tubes. All three pitches are represented, with the values of the normalized, average heat-transfer coefficient of the 30th tube for the pitches of 16, 7.6 and 4 mm approximately 45%, 118%, and 120%, respectively, above the value predicted by Nusselt. As mentioned previously, the wire wrapping makes two separate contributions towards the increase in the heat-transfer coefficient--it thins the condensate film and acts as a condensate drainage channel. When compared with Figure 5.3, Figure 5.5 shows that condensate inundation has less effect on wire-wrapped tubes than it does on a set of smooth tubes and that a wire pitch of 7.6 mm gives the optimal results.

The optimum wire pitch or wire diameter is not simply based on the largest value of h_N/h_1, but also on the actual value of h_1. For example, both 4 mm wire pitch and 7.6 mm wire pitch resulted in about the same h_N/h_1 value (see Figure 5.6). But the h_1 on the tube wrapped with the 7.6 mm wire pitch is about 10 percent greater than the tube with the 4.0 mm wire pitch. Thus, the 7.6 mm wire pitch gave the optimal results for the 1.6-mm-o.d. wire. A more thorough discussion of the point is provided later in this chapter (Section H).

E. THE EFFECT OF INUNDATION ON SMOOTH TUBES WRAPPED WITH 1.0-MM-O.D. WIRE

Three different pitches (8 mm, 6 mm and 4 mm) were tested at this wire diameter. Again, only the graph for the

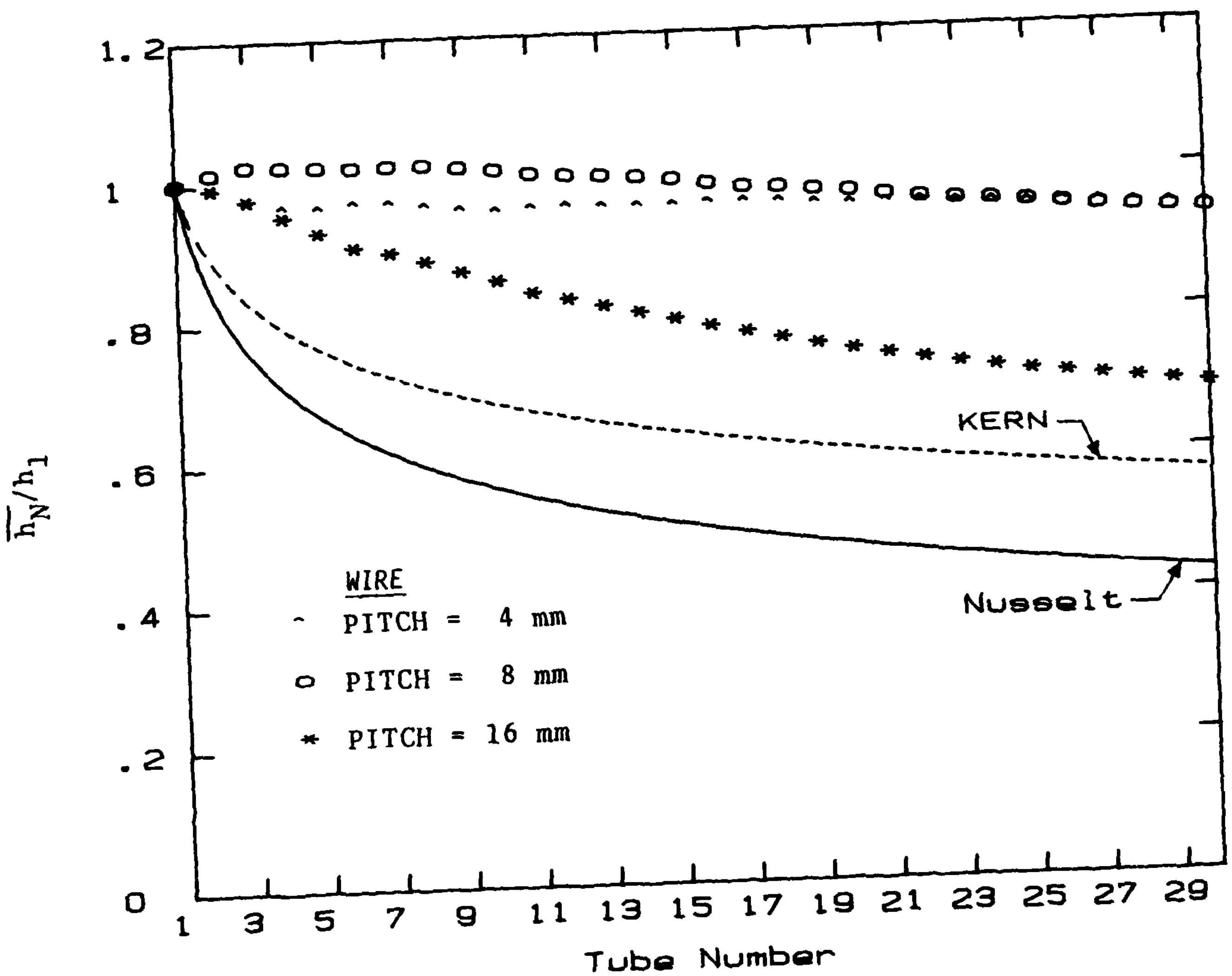

Figure 5.6 Effect of 1.6-mm-o.d. Wire on Inundation (Normalized, Average Heat-Transfer Coefficient)

optimum pitch will be presented for the normalized, local heat-transfer coefficient for a bundle of up to 30 tubes. The graph for a pitch of 4 mm is presented as Figure 5.7. The value for the normalized, local heat-transfer coefficient for the 30th tube is approximately 151% above the value predicted by the Nusselt theory and 71% above the value predicted by the Kern relationship.

Figure 5.8 shows the normalized, average heat-transfer coefficient for a bundle of up to 30 tubes. Again, all three pitches are represented. The values of the normalized, average heat-transfer coefficient of the 30th tube (for the pitches 8, 6 and 4 mm) are approximately 90%, 105% and 117%, respectively, above the value predicted by Nusselt. These graphs again show that this tube configuration is less affected by condensate inundation than the smooth-tube set, and that the optimal wire pitch is 4 mm with this smaller diameter wire.

F. THE EFFECT OF INUNDATION ON SMOOTH TUBES WRAPPED WITH 0.5-MM-O.D. WIRE

Two pitches (4 mm and 2 mm) were tested at this wire diameter. For the normalized, local heat-transfer coefficient for a bundle of up to 30 tubes, only the optimum pitch of 4 mm will be presented. The graph is presented as Figure 5.9. The value for the normalized, local heat-transfer coefficient for the 30th tube is approximately 101% above the value predicted by Nusselt and 37% above the value predicted by the Kern relationship.

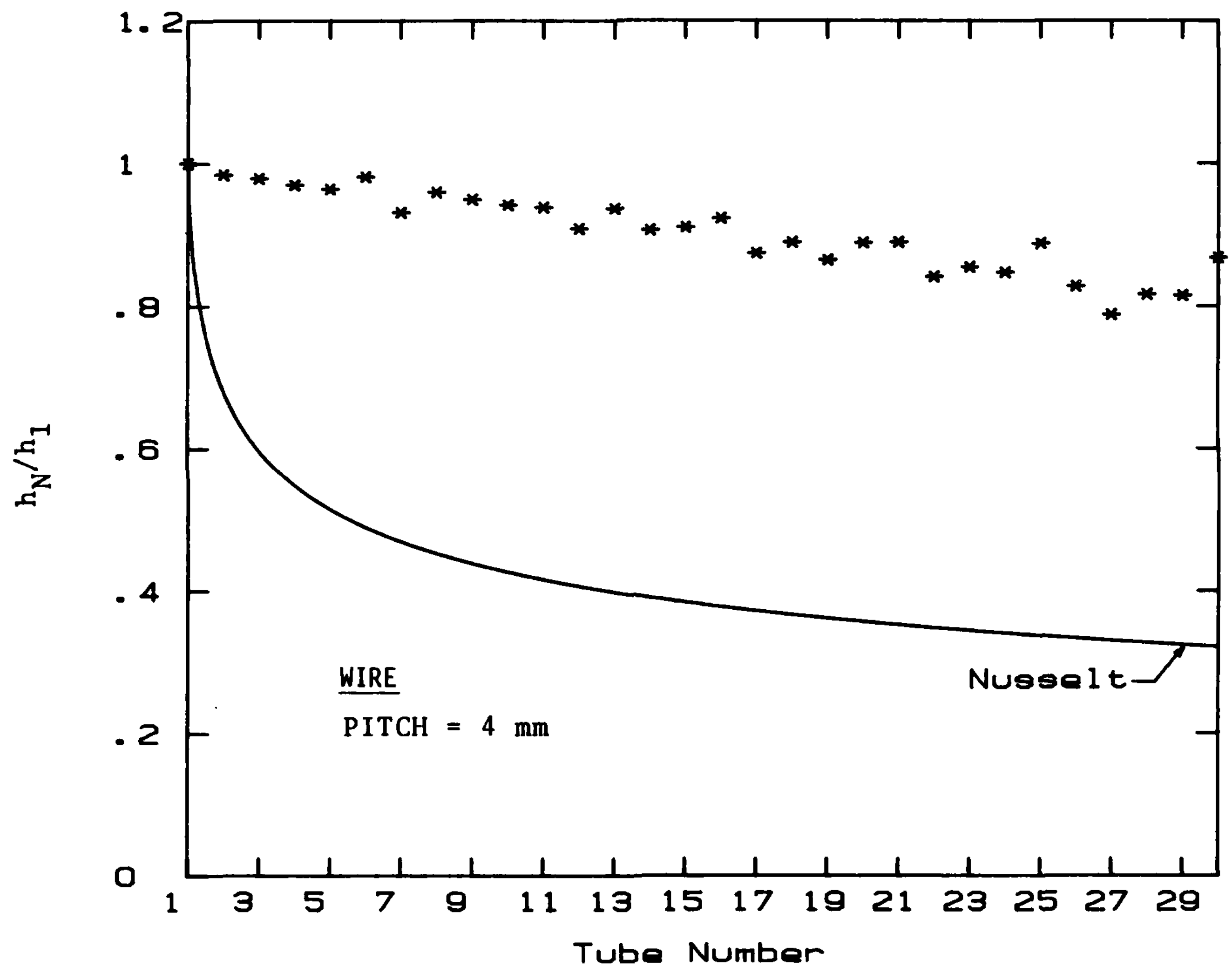

Figure 5.7 Effect of 1.0-mm-o.d. Wire on Inundation (Normalized, Local Heat-Transfer Coefficient)

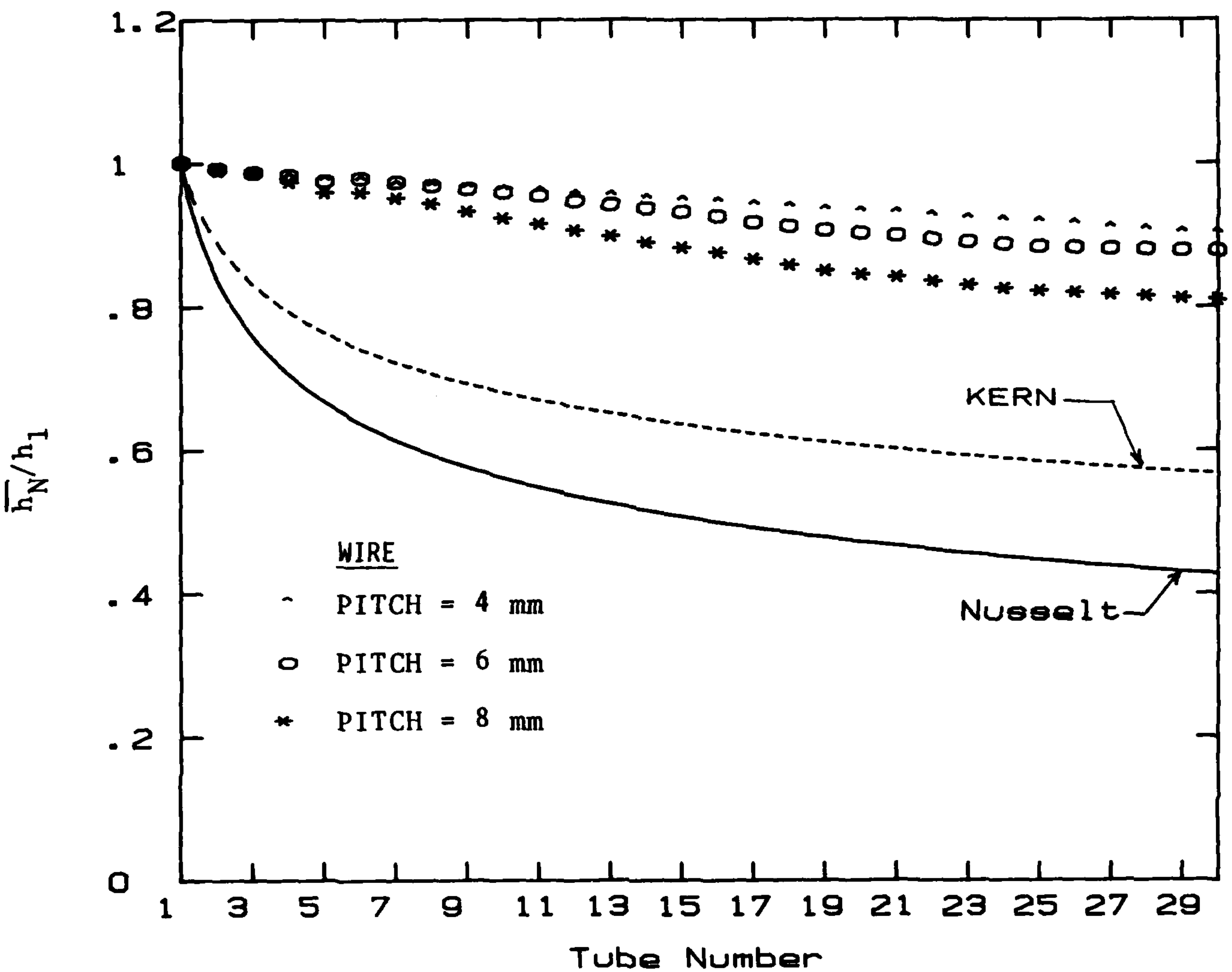

Figure 5.8 Effect of 1.0-mm-o.d. Wire on Inundation (Normalized, Average Heat-Transfer Coefficient)

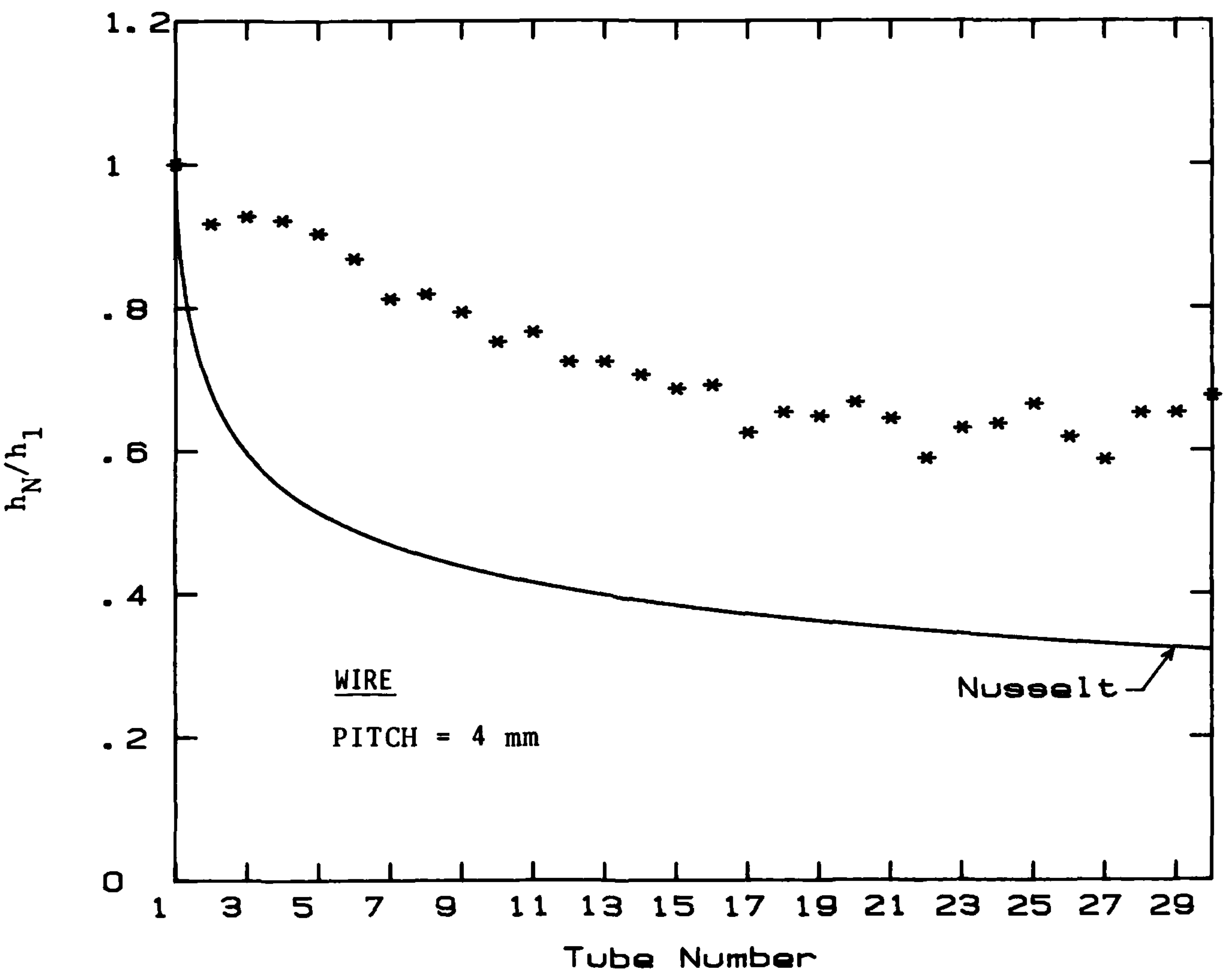

Figure 5.9 Effect of 0.5-mm-o.d. Wire on Inundation (Normalized, Local Heat-Transfer Coefficient)

Figure 5.10 shows the normalized, average heat-transfer coefficient for a bundle of up to 30 tubes. Both of the pitches are represented. The values of the normalized, average heat-transfer coefficient for the 30th tube (for the pitches 4 and 2 mm) are approximately 71% and 80%, respectively, above the value predicted by Nusselt. These graphs also indicate that this tube configuration is not affected by condensate inundation as much as the smooth-tube set.

G. THE EFFECT OF INUNDATION ON SMOOTH TUBES WITH A DROPWISE COATING

A set of smooth tubes with a dropwise coating was tested primarily to observe the effect of inundation. Figure 5.11 shows the normalized, average heat-transfer coefficient for a bundle of 30 tubes. Also included in the figure for comparison are the data for the smooth tube. As is immediately evident from the graph, condensate inundation does not decrease the performance of the dropwise-coated tubes. The ratio of the average outside heat-transfer coefficient of N tubes, divided by the heat-transfer coefficient of the first tube can be seen to rise at first and then remain steady at a value of approximately 1.1.

Since the coating is non-wetting, no large droplets form; rather, the droplets are small when they first form and roll down the side of the tube, as soon as they reach a moderate size. As these droplets are making their descent down the side of the tube, they collect additional droplets until they

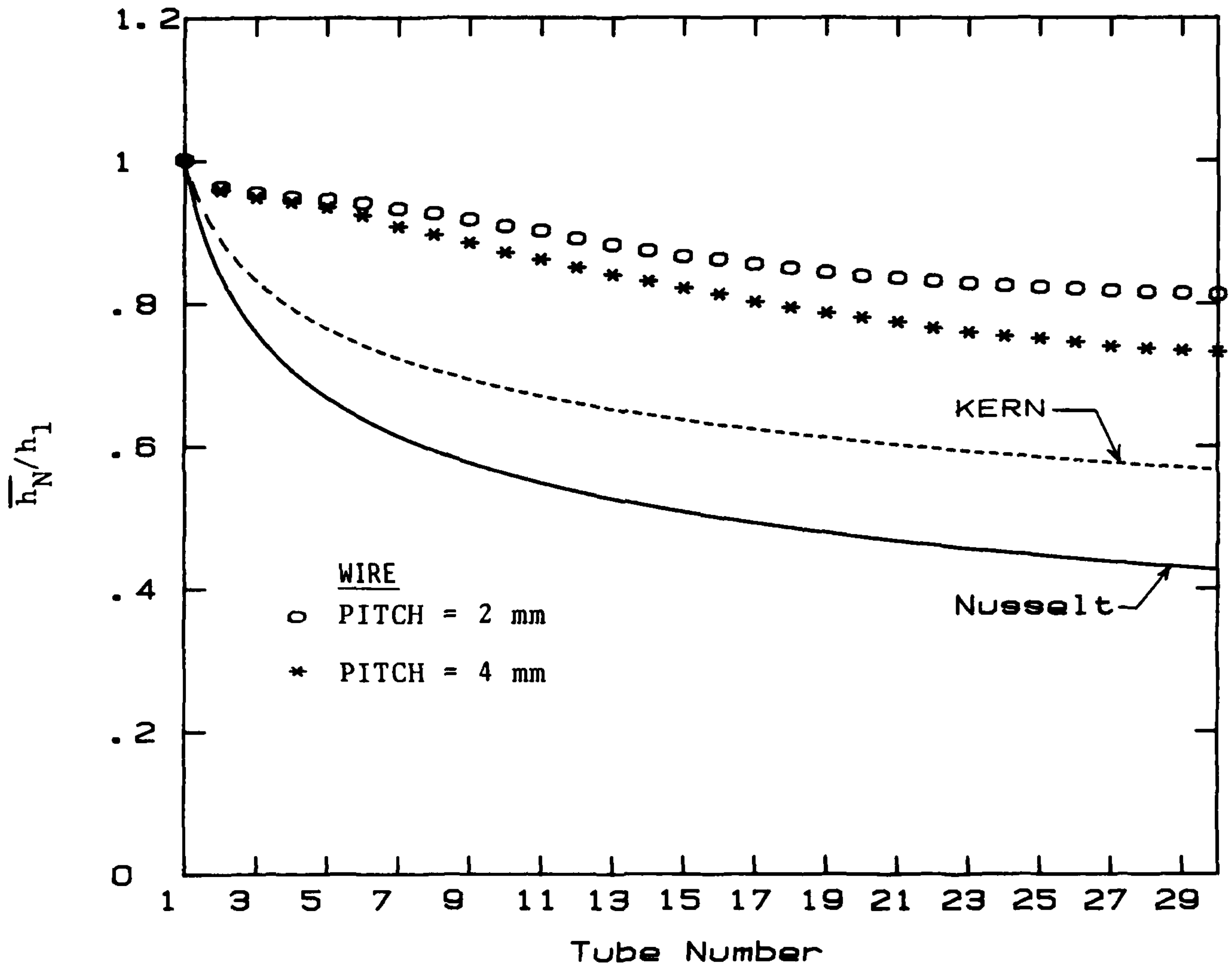

Figure 5.10 Effect of 0.5-mm-o.d. Wire on Inundation (Normalized, Average Heat-Transfer Coefficient)

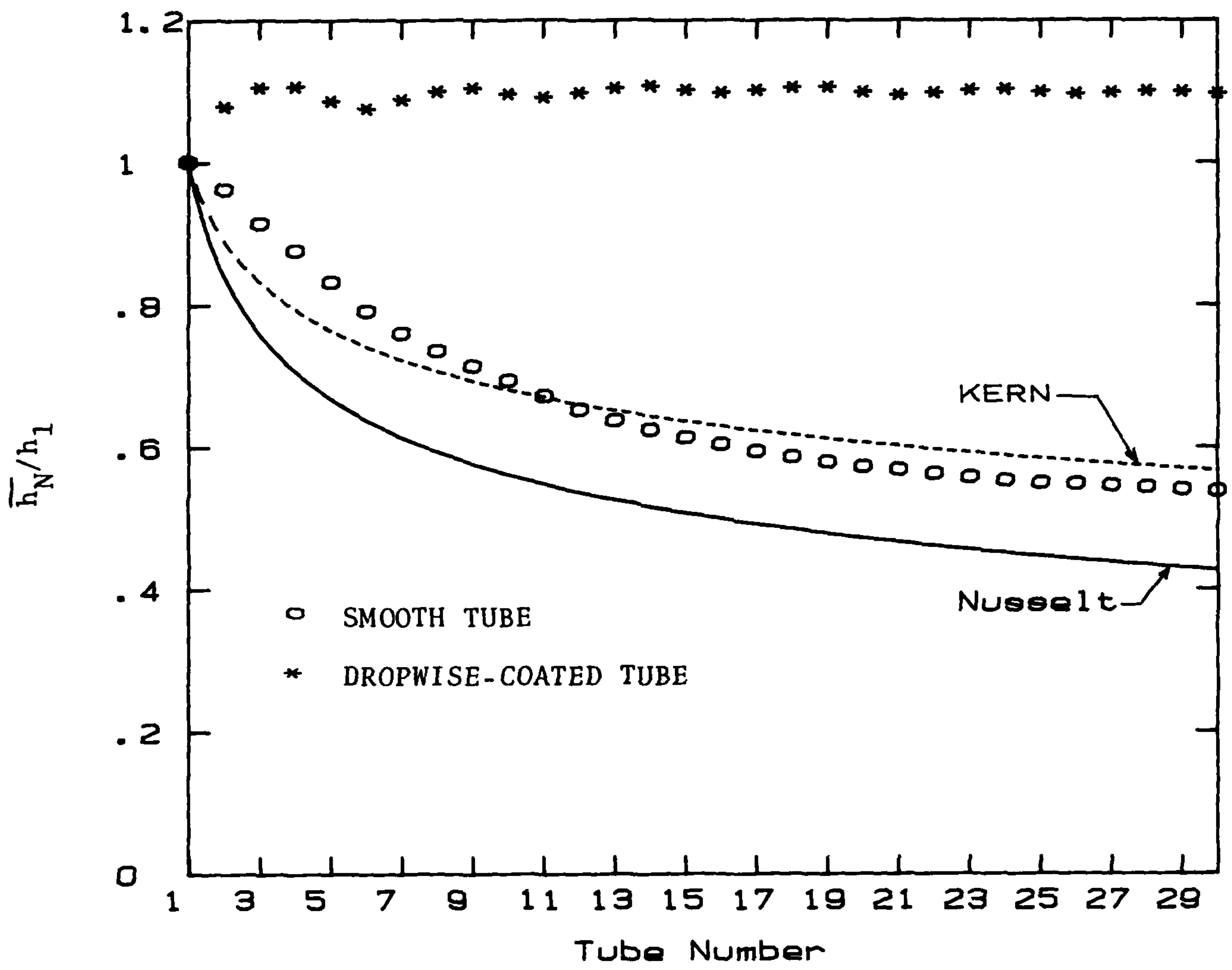

Figure 5.11 Effect of Inundation on a Dropwise Tube Bundle

reach a point where they are able to fall off the tube. As these droplets strike the tubes below, they again collect condensate and act as a sweeper of the condensate across the surface of the tubes below.

H. SUMMARY

Table 3 represents a summary of the results obtained from the data sets presented in this thesis. The column h_1/h_{Nu} is the measure of the local heat-transfer coefficient of the first tube compared to the Nusselt prediction. It can be considered a measure of the effectiveness of the wire-and-pitch combination to thin the condensate film between successive wire wraps. Refer to Figure 5.12 for clarification of this point. The column $\overline{h_{30}}/h_1$ is the measure of the average heat-transfer coefficient for 30 tubes compared to the coefficient for the first tube. This can be considered to be a measure of the effectiveness of the wire-and-pitch combination at handling the condensate drainage. The column $\overline{h_{30}}/h_{Nu}$ is the measure of the average heat-transfer coefficient for 30 tubes compared to the heat-transfer coefficient predicted by the Nusselt theory for a single tube. It can be viewed as a measure of the overall performance of the 30 tube bundle. The last column (labelled s) is the exponent defined in equation (5.1), and is calculated using the least-squares fit for each data run.

As can be seen from the data, it appears that the larger the wire, the better it aids in condensate drainage.

TABLE 3

Data Summary

TUBE SET	WIRE DIAMETER (mm)	WIRE PITCH (mm)	h_1 $(kW/m^2.K)$	h_1/h_{Nu}	$\overline{h_{30}}/h_1$	$\overline{h_{30}}/h_{Nu}$	s^*
1	Smooth tube		12.65	1.193	0.537	0.640	0.183
2a	1.58	16.0	12.32	1.151	0.687	0.791	0.097
b	1.58	7.6	11.36	1.053	0.932	0.981	0.012
c	1.58	4.0	10.41	0.953	0.941	0.897	0.017
3a	1.01	8.0	12.94	1.221	0.810	0.989	0.055
b	1.01	6.0	13.28	1.247	0.877	1.093	0.034
c	1.01	4.0	13.38	1.273	0.904	1.151	0.024
4a	0.50	4.0	15.82	1.504	0.732	1.101	0.082
b	0.50	2.0	13.90	1.294	0.811	1.050	0.061
5	Dropwise-coated tube		10.64	0.970	1.097	1.064	-0.072

* NOTE: Determined by curve fitting the data for tubes 11 through 30.

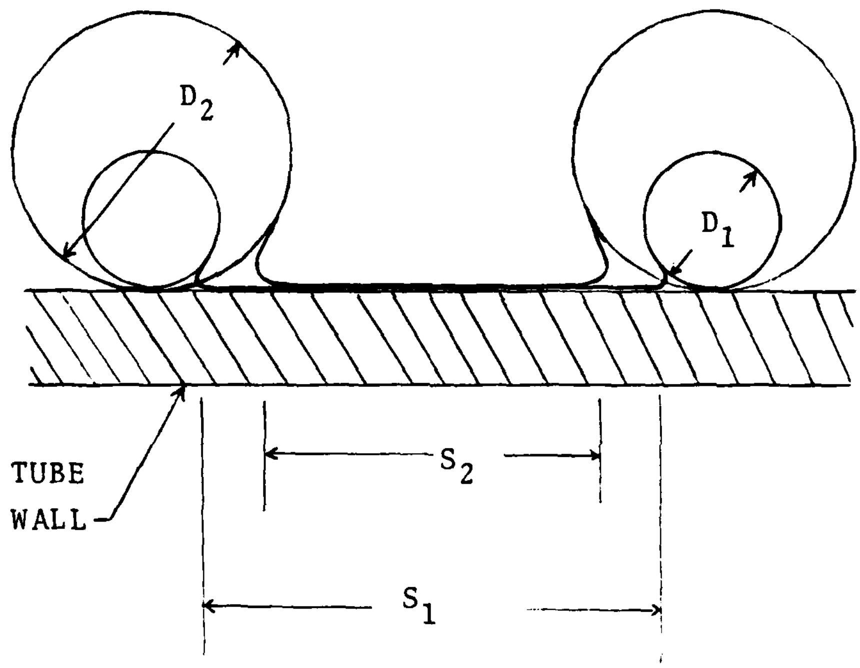

S_1 = Exposed surface for diameter 1.

S_2 = Exposed surface for diameter 2.

Figure 5.12 Effect of Wire Diameter on Condensation

Conversely, the smaller the wire the higher the heat-transfer performance of the first tube. These last two observations are based on a comparison at a 4 mm pitch but with three different wire diameters. The explanation for this is that, for a given pitch, as the wire diameter of the wrap is increased, less and less tube surface area remains exposed to the steam flow. In addition to this, the condensate film thickness may also increase as the wire diameter is increased. Thus, for a given wire pitch, the heat-transfer coefficient of the first tube will increase with a decrease in the wire diameter. On the other hand, the amount of condensate collected around the wire increases with increasing wire diameter (see Figure 5.12). While the surface-tension forces tend to retain liquid at the wire, gravitational forces tend to draw liquid along the wire. As the wire diameter increases, the gravitational forces increase at a faster rate than the surface-tension forces. Therefore, condensate drainage increases with increasing wire diameter.

I. OBSERVATIONS

1. Smooth Tubes

During the data runs, filmwise condensation was observed with no visible indication of dropwise condensation. When the inundation rate was increased, more drops formed along the bottom of the tubes, but the droplet size did not increase noticeably. However, at the higher inundation

conditions there was a noticeable amount of splashing occurring in the test condenser.

2. Wire-Wrapped Tubes

As the steam was condensing on the tubes, the condensate was observed to be drawn to the wire wrap, leaving a thin film between the wires (film thickness was dependent upon the particular wire diameter and pitch). The condensate then ran down the wire and formed droplets on the bottom of the tube. The droplet size was different for each configuration of wire diameter and pitch. For the larger diameter wire, rivulets formed and there was a solid condensate "bridge" from the tubes above to the tubes just below them. As the inundation rate increased, these bridges became more pronounced. It was also noticed that the tendency to splash increased as the inundation rate increased, and was quite noticeable for all of the tube sets tested.

3. Dropwise-Coated Tubes

As was mentioned previously, the condensate droplets from the upper tubes in the bundle act as sweepers of the condensate across the surface of the tubes below them in the tube bundle. During the data run, the condensate collecting on the upper tubes and then falling onto the tubes below was sweeping the lower tubes at such a rate that the droplets forming on the lower tubes never reached a size larger than approximately 2 mm.

VI. CONCLUSIONS

1. The average, outside heat-transfer coefficient for 30 smooth tubes in a vertical column was 64% of the Nusselt coefficient for the first tube in the tube bundle.

2. With wire wrapping, the average, outside heat-transfer performance of the tube bundle is considerably improved. Significant improvements in the outside heat-transfer performance are also possible by utilizing dropwise coatings.

3. The optimum pitch for the 1.6-mm-o.d. wire wrapping occurred at 7.6 mm. With this wire arrangement, the average, outside heat-transfer coefficient for the 30 tubes was 92% of the Nusselt coefficient for the first tube in the tube bundle.

4. The best pitch tested for the 1.0-mm-o.d. wire wrapping occurred at 4 mm. With this wire arrangement, the average, outside heat-transfer coefficient for the 30 tubes was 115% of the Nusselt coefficient for the first tube in the tube bundle.

5. The best pitch tested for the 0.5-mm-o.d. wire wrapping occurred at 4 mm. In this case, the average, outside heat-transfer coefficient for the 30 tubes was 110% of the Nusselt coefficient for the first tube in the tube bundle.

6. In simulating a bundle of 30 tubes coated with a dropwise promoter, the normalized, average, outside heat-transfer coefficient increased by approximately 10% over the value for the top tube in the bundle.

VII. RECOMMENDATIONS

A. TEST APPARATUS MODIFICATIONS

The modifications listed below should be considered prior to continued use of the test apparatus:

1. Redesign the test condenser to reduce the possibility of the steam bypassing the active test condenser tubes.

2. Install a larger heating system in the perforated-tube water supply tank or modify the existing heating system to increase the slow response of the heating system.

The modifications listed below would be beneficial to the operation of the test apparatus but are not necessary for proper operation:

1. Redesign the existing controls so that the test apparatus is controllable from a single panel.

2. Redesign the test condenser hotwell to provide a more accurate measure of the condensate collection rate.

B. ADDITIONAL TESTS TO CONDUCT

The following additional tests would be important in the continuation of this investigation:

1. Conduct tests with additional wire pitches for the 1.0-mm-diameter wire to determine the optimum wire pitch.

2. Conduct tests using other dropwise coatings.

3. Conduct tests with the commercially-available finned tubes.

4. Conduct additional tests to determine the effect of vapor shear on the outside heat-transfer coefficient.

APPENDIX A

SAMPLE CALCULATIONS

A. A sample calculation is performed in this section to illustrate the solution procedure used in the data-reduction program presented in Appendix C. The calculations are limited to the first tube in the bundle only. All thermophysical properties were determined from the Tables in Reference 32.

EXPERIMENTAL CONDITIONS:

Pressure Condition	Atmospheric
Inundation Condition	5 tubes
Inlet Temperature of Cooling Water	24.10 °C
Outlet Temperature of Cooling Water	28.32 °C
Saturation Temperature	100.65 °C
Cooling Water Rotameter Setting	21.7%

1. Determination of Average Bulk Temperature

$$T_b = (T_{ci} + T_{co})/2$$

$$T_b = (24.10 + 28.32)/2$$

$$T_b = 26.21 \text{ °C}$$

2. Thermophysical Properties (evaluated at T_b)

$$P_r = 5.83$$

$$\rho_c = 997 \text{ kg/m}^3$$

$$\mu_c = 855 \times 10^{-6} \ \mathrm{N \cdot s/m^2}$$

$$C_{pc} = 4.179 \ \mathrm{kJ/kg \cdot K}$$

$$k_c = 618 \times 10^{-3} \ \mathrm{W/m \cdot K}$$

$$\dot{m}_c = 0.243 \ \mathrm{kg/s}$$

4. Determination of Cooling Water Velocity

$$V_c = \dot{m}_c/(\rho_c \cdot A_i)$$

$$V_c = (0.243)/(997) \cdot (1.56 \times 10^{-4})$$

$$V_c = 1.56 \ \mathrm{m/s}$$

5. Determination of Reynolds Number

$$Re = (\rho_c \ V_c \ D_i)/\mu_c$$

$$Re = (997)(1.56)(.0141)/855 \times 10^{-6}$$

$$Re = 25{,}649$$

6. Determination of Heat Transfer

$$Q = \dot{m}_c(T_{co} - T_{ci}) \ C_{pc}$$

$$Q = 0.243(28.32 - 24.1)4179$$

$$Q = 4285 \ \mathrm{W}$$

7. <u>Determination of Heat Flux</u>

$$q = Q/(\pi\ D_o\ L)$$

$$q = 4285/\pi(0.015875)(0.305)$$

$$q = 281{,}700\ W/m^2$$

8. <u>Determination of Nusselt Coefficient</u>

$$h_{Nu} = 0.651 \left[\frac{k_f^3\ \rho_f^2\ h_{fg}\ (9.81)}{\mu_f\ D_o\ q}\right]^{1/3}$$

Assume:

$$T_f = T_{sat}$$

$$T_f = 100.65\ °C$$

$$\rho_f = 957.8\ kg/m^3$$

$$h_{fg} = 2255\ J/kg$$

$$k_f = 680.52\ W/m \cdot K$$

$$\mu_f = 277.6 \times 10^{-6}\ N \cdot s/m^2$$

$$h_{Nu} = 0.651 \left[\frac{(680.52\times10^{-3})^3 (957.8)^2 (2255\times10^3)(9.81)}{(277.6\times10^{-6})(0.015875)(281{,}700)}\right]^{1/3}$$

$$h_{Nu} = 11{,}243.6\ W/m^2 \cdot K$$

9. <u>Determination of $T_{f,c}$</u>

$$T_{f,c} = T_{sat} - q/(2 \cdot h_{Nu})$$

$$T_{f,c} = 100.65 - 281{,}700/2(11{,}243.6)$$

$$T_{f,c} = 88.12\ °C$$

10. <u>Thermophysical Properties</u>

$$k_f = 674.6 \times 10^{-3}\ W/m \cdot K$$

$$\rho_f = 966\ kg/m^3$$

$$\mu_f = 320.3 \times 10^{-6}\ N \cdot s/m^2$$

$$h_{fg} = 2288.3 \times 10^3\ J/kg$$

11. <u>Determination of Nusselt Coefficient</u>

$$h_{Nu} = 0.651 \left[\frac{k_f^3\ \rho_f^2\ h_{fg}\ 9.81}{\mu_f\ D_o\ q} \right]^{1/3}$$

$$h_{Nu} = 0.651 \left[\frac{(674.6 \times 10^{-3})^3 (966)^2 (2288.3 \times 10^3)(9.81)}{(320.3 \times 10^{-6})(0.015875)(281{,}700)} \right]^{1/3}$$

$$h_{Nu} = 10{,}739.6\ W/m^2K$$

12. <u>Determination of $T_{f,c}$</u>

$$T_{f,c} = T_{sat} - q/(2 \cdot h_{Nu})$$

$$T_{f,c} = 100.65 - 281{,}700/(2)(10{,}739.6)$$

$$T_{f,c} = 87.53\ °C$$

13. <u>Determination of Logarithmic Mean Temperature</u>

$$LMTD = (T_{co} - T_{ci})/\ell n\left(\frac{T_{sat} - T_{ci}}{T_{sat} - T_{co}}\right)$$

$$LMTD = (28.32 - 24.10)/\ell n\left(\frac{100.65 - 24.10}{100.65 - 28.32}\right)$$

$$LMTD = 74.42\ °C$$

14. <u>Determination of Overall Heat-Transfer Coefficient</u>

$$U_o = q/LMTD$$

$$U_o = 281{,}700/74.42$$

$$U_o = 3785.3\ W/m^2 \cdot K$$

15. <u>Determination of Inside Heat-Transfer Coefficient</u>

Assume:

$$C_f = 1.1$$

$$C_i = 0.028$$

$$h_i = \frac{k_c}{D_i} C_i\ Re^{0.8}\ Pr^{0.333}\ C_f$$

$$h_i = \frac{0.618}{0.0141}(0.028)(25{,}649)^{0.8}(5.83)^{0.333}(1.1)$$

$$h_i = 8181\ W/m^2K$$

16. Determination of Inner Wall Temperature

$$T_w = T_b + q\ D_o/(h_i\ D_i)$$

$$T_w = 26.21 + (281{,}700)(0.015875)/(8181)(0.0141)$$

$$T_w = 64.98\ °C$$

17. Determination of μ_w at the Average Wall Temperature

$$\mu_w = 433 \times 10^{-6}\ N \cdot s/m^2$$

18. Determination of Correction Factor

$$C_{f,c} = (\mu_c/\mu_w)^{0.14}$$

$$C_{f,c} = 1.1$$

19. Determination of Outisde Heat-Transfer Coefficient

$$h_o = \frac{1}{\frac{1}{U_o} - \frac{D_o}{D_i\ h_i} - R_w}$$

$$h_o = \frac{1}{\frac{1}{3785.3} - \frac{0.015875}{(0.0141)(8181)} - 0.000042925}$$

$$h_o = 11{,}957\ W/m^2K$$

APPENDIX B

UNCERTAINTY ANALYSIS

The uncertainty analysis performed for this thesis is based on the development described in Kline and McClintock [Ref. 33]. Kanakis [Ref. 12] employed this development and derived the expressions for uncertainty in the variables of this thesis also. In this thesis, the results presented by Kanakis [Ref. 12] in Appendix C will be utilized, but where necessary, corrections will be pointed out.

A. UNCERTAINTY IN THE COOLING WATER VELOCITY

$$\frac{\delta V_c}{V_c} = \left[\left(\frac{\delta \dot{m}_c}{\dot{m}_c}\right)^2 + \left(\frac{\delta \rho_c}{\rho_c}\right)^2 + \left(\frac{\delta A_i}{A_i}\right)^2 \right]^{1/2}$$

with the following uncertainties assigned:

$$\delta \dot{m}_c = \pm\ 0.01 \text{ kg/s}$$

$$\delta \rho_c = \pm\ 3 \text{ kg/m}^3$$

$$\delta A_i = \pm\ 0.00000022 \text{ m}^2$$

B. UNCERTAINTY IN THE REYNOLDS NUMBER

$$\frac{\delta Re}{Re} = \left[\left(\frac{\delta \rho_c}{\rho_c}\right)^2 + \left(\frac{\delta V_c}{V_c}\right)^2 + \left(\frac{\delta D_i}{D_i}\right)^2 + \left(\frac{\delta \mu_c}{\mu_c}\right)^2 \right]^{1/2}$$

with the following uncertainties assigned:

$$\delta\rho_c = \pm\ 3\ \mathrm{kg/m^3}$$

δV_c as calculated in Section A

$$\delta D_i = \pm\ 0.0001\ \mathrm{m}$$

$$\delta\mu_c = \pm\ 10 \times 10^{-6}\ \mathrm{N\cdot s/m^2}$$

C. UNCERTAINTY IN HEAT TRANSFER

$$\frac{\delta Q}{Q} = \left[\left(\frac{\delta \dot{m}_c}{\dot{m}_c}\right)^2 + \left(\frac{\delta\ T_{co}}{T_{co}-T_{ci}}\right)^2 + \left(\frac{\delta\ T_{ci}}{T_{co}-T_{ci}}\right)^2 + \left(\frac{\delta C_{pc}}{C_{pc}}\right)^2 \right]^{1/2}$$

with the following uncertainties assigned:

$$\delta\dot{m}_c = \pm\ 0.01\ \mathrm{kg/s}$$

$$\delta T_{co} = \pm\ 0.025\ ^\circ\mathrm{C}$$

$$\delta T_{ci} = \pm\ 0.025\ ^\circ\mathrm{C}$$

$$\delta C_{pc} = \pm\ 2\ \mathrm{J/kg\cdot C}$$

D. UNCERTAINTY IN THE HEAT FLUX

$$\frac{\delta q}{q} = \left[\left(\frac{\delta Q}{Q}\right)^2 + \left(\frac{\delta D_o}{D_o}\right)^2 + \left(\frac{\delta L}{L}\right)^2 \right]^{1/2}$$

with the following uncertainties assigned:

δQ as calculated in Section C

δD_o = $\pm$ 0.0001 m

δL = $\pm$ 0.001 m

E. UNCERTAINTY IN h_{Nu}

$$\frac{\delta h_{Nu}}{h_{Nu}} = \left[\left(\frac{\delta k_f}{k_f}\right)^2 + \left(\frac{2}{3}\,\frac{\delta \rho_f}{\rho_f}\right)^2 + \left(\frac{1}{3}\,\frac{\delta h_{fg}}{h_{fg}}\right)^2 + \left(\frac{1}{3}\,\frac{\delta g}{g}\right)^2 + \left(\frac{1}{3}\,\frac{\delta \mu_f}{\mu_f}\right)^2 + \left(\frac{1}{3}\,\frac{\delta D_o}{D_o}\right)^2 + \left(\frac{1}{3}\,\frac{\delta q}{q}\right)^2 \right]^{1/2}$$

with the following uncertainties assigned:

δk_f = $\pm$ 0.0005 W/m·K

$\delta \rho_f$ = $\pm$ 3 kg/m^3

δh_{fg} = $\pm$ 0.12 J/kg

δg = $\pm$ 0.0005 m/s

$\delta \mu_f$ = $\pm$ 4.9 $\times 10^{-6}$ N·s/m^2

δD_o = $\pm$ 0.0001 m

δq as calculated in Section D

F. UNCERTAINTY IN $T_{f,c}$

$$\frac{\delta T_{f,c}}{T_{f,c}} = \left[\left(\frac{\delta T_{sat}}{T_{sat}}\right)^2 + \left(\frac{\delta q}{q}\right)^2 + \left(\frac{\delta h_{Nu}}{h_{Nu}}\right)^2 \right]^{1/2}$$

with the following uncertainties assigned:

$\delta T_{sat} = \pm\ 0.025\ °C$

δq as calculated in Section D

δh_{Nu} as calculated in Section E

G. UNCERTAINTY IN LOGARITHMIC-MEAN-TEMPERATURE DIFFERENCE

$$\frac{\delta LMTD}{LMTD} = \left[\left(\frac{\delta T_{sat}(T_{co} - T_{ci})}{(T_{sat}-T_{ci})(T_{sat}-T_{co})\ln\left(\frac{T_{sat}-T_{ci}}{T_{sat}-T_{co}}\right)} \right)^2 \right.$$

$$+ \left(\frac{\delta T_{co}}{(T_{sat}-T_{co})\ln\left(\frac{T_{sat}-T_{ci}}{T_{sat}-T_{co}}\right)} \right)^2$$

$$\left. + \left(\frac{\delta T_{ci}}{(T_{sat}-T_{ci})\ln\left(\frac{T_{sat}-T_{ci}}{T_{sat}-T_{co}}\right)} \right)^2 \right]^{1/2}$$

with the following uncertainties assigned:

$$\delta T_{sat} = \pm\ 0.025\ °C$$

$$\delta T_{co} = \pm\ 0.025\ °C$$

$$\delta T_{ci} = \pm\ 0.025\ °C$$

H. UNCERTAINTY IN OVERALL HEAT-TRANSFER COEFFICIENT

$$\frac{\delta U_o}{U_o} = \left[\left(\frac{\delta q}{q}\right)^2 + \left(\frac{\delta LMTD}{LMTD}\right)^2 \right]^{1/2}$$

with the following uncertainties assigned:

δq as calculated in Section D

$\delta LMTD$ as calculated in Section G

I. UNCERTAINTY IN INSIDE HEAT-TRANSFER COEFFICIENT

$$\frac{\delta h_i}{h_i} = \left[\left(\frac{\delta k_c}{k_c}\right)^2 + \left(\frac{\delta D_i}{D_i}\right)^2 + \left(\frac{0.8\ \delta Re}{Re}\right)^2 + \left(\frac{0.333\ \delta Pr}{Pr}\right)^2 + \left(\frac{\delta C_i}{C_i}\right)^2 + \left(\frac{0.14\delta(\mu_c/\mu_w)}{\mu_c/\mu_w}\right)^2 \right]^{1/2}$$

with the following uncertainties assigned:

$$\delta k_c = \pm\ 0.0005\ W/m{\cdot}K$$

$$\delta D_i = \pm\ 0.0001\ m$$

δRe as calculated in Section B

$$\delta P_r = \pm 0.063$$

$$\delta C_i = \pm 0.0001$$

$$\delta(\mu_c/\mu_w) = \pm 4.9 \times 10^{-6} \ \mathrm{N \cdot s/m^2}$$

J. UNCERTAINTY IN TEMPERATURE DIFFERENCE

$$\frac{\delta DT}{DT} = \left[\left(\frac{\delta q}{q}\right)^2 + \left(\frac{\delta h_i}{h_i}\right)^2 + \left(\frac{\delta D_o}{D_o}\right)^2 + \left(\frac{\delta D_i}{D_i}\right)^2 \right]^{1/2}$$

with the following uncertainties assigned:

δq as calculated in Section D

δh_i as calculated in Section I

$$\delta D_o = \pm 0.0001 \ \mathrm{m}$$

$$\delta D_i = \pm 0.0001 \ \mathrm{m}$$

K. UNCERTAINTY IN OUTSIDE HEAT-TRANSFER COEFFICIENT

$$\frac{\delta h_o}{h_o} = \left[\left(\frac{\delta U_o}{U_o^2 \left(\frac{1}{U_o} - R_w - \frac{D_o}{D_i \, h_i} \right)} \right)^2 + \left(\frac{\delta R_w}{\frac{1}{U_o} - R_w - \frac{D_o}{D_i \, h_i}} \right)^2 + \left(\frac{\left(\frac{D_o}{D_i \, h_i} \right) \left(\frac{\delta h_i}{h_i} \right)}{\frac{1}{U_o} - R_w - \frac{D_o}{D_i \, h_i}} \right)^2 \right]^{1/2}$$

with the following uncertainties assigned:

δU_o as calculated in Section H

$\delta R_w = \pm 0.00001 \ m^2 \cdot K/W$

δh_i as calculated in Section I

For the data presented in Appendix A, the following uncertainties are the result:

		quantity		uncertainty
V_c	=	1.56	±	0.064 m/s
Re	=	25,649	±	1112

		quantity		uncertainty
Q	=	4258	±	169 w
q	=	281,700	±	12,010 W/m^2
h_{Nu}	=	11,243.6	±	163.4 $W/m^2 \cdot K$
$T_{f,c}$	=	88.12	±	4.0 °C
LMTD	=	74.42	±	0.625 °C
U_o	=	3785.3	±	164.48 $W/m^2 \cdot K$
h_i	=	8181	±	292.6 $W/m^2 \cdot K$
DT	=	38.77	±	2.19 °C
h_o	=	11,957	±	2287 $W/m^2 \cdot K$

APPENDIX C

DATA REDUCTION AND PLOTTING PROGRAMS

```
1000! FILE NAME: DRP3
1005! DATE:      May 9, 1984
1010!
1015  BEEP
1020  PRINTER IS 1
1025  PRINT USING "4X,""Select Option:"""
1030  PRINT USING "6X,""0 Taking data or re-processing previous data"""
1035  PRINT USING "6X,""1 Plotting previous data"""
1040  PRINT USING "6X,""2 Computing exponent for experimental data"""
1045  PRINT USING "6X,""3 Plotting on LOG-LOG"""
1050  PRINT USING "6X,""4 Labelling"""
1055  INPUT Iop
1060  IF Iop=0 THEN CALL Main
1065  IF Iop=1 THEN CALL Plot
1070  IF Iop=2 THEN CALL Expo
1075  IF Iop=3 THEN CALL Lplot
1080  IF Iop=4 THEN CALL Label
1085  END
1090  SUB Main
1095  COM /Ci/ C(7)
1100  DIM Tci(2),Tco(4,2),Ti(4),Mft(4),Vw(4),Ho(4)
1105  DIM To(4),Ts(1),Tb(4),R3(4),R4(4),S3(4),S4(4),Fc(4),Mfi(4),Mfs(4)
1110!
1115! ASSIGN COEFFICIENTS FOR THE 8-TH ORDER
1120! POLYNOMIAL FOR TYPE-T (COPPER-CONSTANTAN)
1125! THERMOCOUPLES
1130  DATA 0.10086091,25727.94369,-767345.8295,78025595.81
1135  DATA -9247486589,6.97688E+11,-2.66192E+13,3.94078E+14
1140  READ C(*)
1145!
1150! ASSIGN CONSTANTS FOR ROTAMETER CALIBRATION
1155! LINES (kg/min)
1160!
1165  DATA -1.256E-4,5.866E-3,2.456E-4,-3.352E-3,-5.878E-4
1170  DATA 1.121E-2,1.237E-2,1.221E-2,1.233E-2,1.232E-2
1175  READ Mfi(*),Mfs(*)
1180!
1185! ASSIGN SIEDER-TATE COEFFICIENT AND EXPONENT
1190! FOR REYNOLDS NUMBER
1195  Ex=.8
1200!
1205! ASSIGN GEOMETRIC VARIABLES
1210  Di=.0141       ! Inner diameter (m)
1215  Do=.015875     ! Outer diameter (m)
1220  Ktm=21.9       ! Thermal conductivity of titanium (W/m-K)
1225  L=.305         ! Condensing length (m)
1230  Pt=Do*1.5      ! Transverse tube pitch-to-diameter ratio
1235!
1240! COMPUTE THE MEAN STEAM FLOW AREA IN THE TEST CONDENSER (m^2)
1245  Af=(Pt^2-PI*Do^2/4)/Pt*2*L
1250!
1255! COMPUTE INSIDE AREA AND WALL RESISTANCE
1260  Ai=PI*Di^2/4
1265  Rw=Do*LOG(Do/Di)/(2*Ktm)
1270!
1275  PRINTER IS 701
1280  CLEAR 709
1285  BEEP
1290  INPUT "ENTER MONTH, DATE, AND TIME (MM:DD:HH:MM:SS)",Time$
```

```
1295  OUTPUT 709:"TD":Time$
1300  Sgy=0
1305  Sgf=0
1310  Sgyf=0
1315  Sgf2=0
1320  BEEP
1325  INPUT "VAPOR SHEAR DATA (1=Y,0=N)?",Ivd
1330  IF Ivd=0 THEN
1335  BEEP
1340  INPUT "ENTER OUTPUT MODE (1=SHORT,0=LONG)",Jop
1345  END IF
1350  BEEP
1355  INPUT "ENTER THE INPUT MODE (1=3054A,2=FILE)",Im
1360  IF Im=2 THEN
1365  BEEP
1370  INPUT "ENTER THE NAME OF THE EXISTING DATA FILE",Olddata$
1375  PRINT USING "10X,""This analysis is for data file "",10A":Olddata$
1380  BEEP
1385  INPUT "ENTER 1 IF PROCESSING 1983 DATA",Idt
1390  ASSIGN @File2 TO Olddata$
1395  END IF
1400  IF Im=1 THEN
1405  BEEP
1410  INPUT "GIVE A NAME FOR THE DATA FILE TO BE CREATED",Newdata$
1415  CREATE BDAT N    ata$,?5
1420  ASSIGN @File'    Ne   ata$
1425  END IF
1430  BEEP
1435  INPUT "GIVE A NAME FOR THE OUTPUT FILE",File_out$
1440  BEEP
1445  INPUT "ENTER TUBE TYPE (0=PLAIN,1=ROPED)",Itt
1450  IF Itt=0 THEN
1455  PRINT USING "10X,""Tube type              : Plain """
1460  Ci=.028
1465  END IF
1470  IF Itt=1 THEN
1475  PRINT USING "10X,""Tube type              : Roped """
1480  Ci=.057
1485  END IF
1490  PRINT USING "10X,""Sieder-Tate constant = "",Z.4D":Ci
1495  BEEP
1500  INPUT "ENTER THE INUNDATION CONDITION (1=5 TUBES, 2=30 TUBES)",Mi
1505  IF Mi=2 THEN PRINT "            Inundation condition : 30 TUBES"
1510  IF Mi=1 THEN PRINT "            Inundation condition : 5 TUBES"
1515  IF Ivd=0 THEN
1520  BEEP
1525  INPUT "WANT TO IN       VAPOR SHEAR (1=Y,0=N)?",Ivs
1530  IF Ivs=1 THEN
1535  BEEP
1540  INPUT "ENTER B-VALUE FOR VAPOR SHEAR CORRELATION",B
1545  BEEP
1550  INPUT "ENTER EX  NENT FOR VAPOR-SHEAR CORRELATION",Nvs
1555  END IF
1560  END IF
1565  CREATE BDAT File_out$,6
1570  ASSIGN @File3 TO File_out$
1575  Ja=0
1580  Nrun=0
1585  FOR I=0 TO 4
1590  S3(I)=0.
1595  S4(I)=0.
```

```
1600  NEXT I
1605  IF Im=1 THEN
1610  BEEP
1615  INPUT "ENTER MANOMETER READINGS (HLW,HLM,HRW,HRM)",Hlw,Hlm,Hrw,Hrm
1620  OUTPUT @File1:Hlw,Hlm,Hrw,Hrm
1625  ELSE
1630  IF Idt=0 THEN ENTER @File2:Hlw,Hlm,Hrw,Hrm
1635  END IF
1640  Dp=Hlm-Hrm+(Hlw-Hlm-Hrw+Hrm)/13.5
1645  Mdot=FNMdot(Dp)
1650  Nrun=Nrun+1
1655  OUTPUT 709:"TD"
1660  ENTER 709:Time$
1665  IF Ivd=0 AND Jop=0 THEN PRINT " "
1670  IF Nrun=1 THEN
1675  PRINT USING "10X,""Month, date, and time: "",15A";Time$
1680  PRINT
1685  END IF
1690  IF Im=2 THEN Rdf
1695  BEEP
1700  INPUT "ENTER FLOW METER READINGS (AS PERCENTAGES)",Fm1,Fm2
1705  DISP "START COLLECTING CONDENSATE"
1710  BEEP
1715  WAIT 20
1720  OUTPUT 709:"AR AF0 AL19"
1725  OUTPUT 722:"F1 R1 T1 Z1 FL1"
1730!
1735! READ INLET WATER TEMPERATURES
1740!
1745  FOR I=0 TO 2
1750  OUTPUT 709:"AS SA"
1755  ENTER 722:Tci(I)
1760  CALL Tvsv(Tci(I))
1765  Tci(I)=FNTemp(Tci(I),I)
1770  NEXT I
1775!
1780! READ OUTLET WATER TEMPERATURES
1785!
1790  Ii=2
1795  FOR I=0 TO 4
1800  IF I=0 OR I=3 THEN
1805  Iu=2
1810  ELSE
1815  Iu=1
1820  END IF
1825  FOR J=0 TO Iu
1830  Ii=Ii+1
1835  OUTPUT 709:"AS SA"
1840  ENTER 722:Tco(I,J)
1845  CALL Tvsv(Tco(I,J))
1850  Tco(I,J)=FNTemp(Tco(I,J),Ii)
1855  NEXT J
1860  NEXT I
1865!
1870! READ STEAM TEMPERATURES
1875!
1880  FOR I=15 TO 16
1885  OUTPUT 709:"AS SA"
1890  ENTER 722:Ts(I-15)
1895  CALL Tvsv(Ts(I-15))
1900  Ts(I-15)=FNTemp(Ts(I-15),I)
```

```
1905  NEXT I
1910!
1915! READ CONDENSATE TEMPERATURE
1920!
1925  OUTPUT 709:"AS SA"
1930  ENTER 722:Tcon
1935  CALL Tvsv(Tcon)
1940  Tcon=FNTemp(Tcon,17)
1945!
1950! READ VAPOR TEMPERATURE
1955!
1960  OUTPUT 709:"AS SA"
1965  ENTER 722:Tv
1970  CALL Tvsv(Tv)
1975  Tv=FNTemp(Tv,18)
1980!
1985! READ VAPOR PRESSURE
1990!
1995  OUTPUT 709:"AS SA"
2000  ENTER 722:P_volts
2005!
2010! COMPUTE AVERAGE WATER TEMPERATURES AT INLET
2015!
2020  Ti(0)=Tci(0)
2025  Ti(1)=(Tci(0)+Tci(1))*.5
2030  Ti(2)=Tci(1)
2035  Ti(3)=(Tci(1)+Tci(2))*.5
2040  Ti(4)=Tci(2)
2045!
2050! COMPUTE AVERAGE WATER TEMPERATURES AT OUTLET
2055!
2060  FOR I=0 TO 4
2065  IF I=0 OR I=3 THEN
2070  To(I)=(Tco(I,0)+Tco(I,1)+Tco(I,2))*.3333
2075  ELSE
2080  To(I)=(Tco(I,0)+Tco(I,1))*.5
2085  END IF
2090  NEXT I
2095  Tsa=(Ts(0)+Ts(1))*.5
2100  Pvap=FNPvsv(P_volts)
2105  Tsat=FNTvsp(Pvap*133.322)
2110  Dsup=Tv-Tsat
2115!
2120! READ INFORMATION FOR CONDENSATE FLOW RATE
2125!
2130  IF Ivd=0 THEN
2135  BEEP
2140  INPUT "ENTER INITIAL AND FINAL LEVELS IN HOT WELL 1",H1,H2
2145  Dh=H2-H1
2150  IF Nrun MOD 5=1 THEN Msum=0
2155  Mf1=540.4836*Dh
2160  Md1=Mf1*FNRhow(Tsat-10)*1.0E-6/60
2165  Msum=Msum+Mf1
2170  IF Mi=2 AND Nrun<>30 AND Nrun MOD 5=0 THEN
2175  Mave=Msum/5
2180  Set=(Mave*FNRhow(Tsat-10)/10^6+.03238)/.042132
2185  END IF
2190!
2195 Rdf: !
2200!
2205  IF Ivd=0 AND Jop=0 THEN
```

```
2210  PRINT USING "10X,""Run number = "",DD";Nrun
2215  PRINT "           Tube #          :   1        2        3        4        5"
2220  END IF
2225  END IF
2230  IF Ivd=1 AND Nrun=1 THEN
2235  PRINT USING "10X,""Data #     Vv      Retp        Nuc       Y        F"""""
2240  END IF
2245  IF Im=2 THEN
2250  IF Nrun MOD 5=1 AND Mi=2 AND Nrun>5 THEN ENTER @File2;Fpt
2255  ENTER @File2;Ti(*),To(*),Tsa,Tcon,Tv,Pvap,Tsat,Dsup,Fm1,Fm2
2260  ENTER @File2;H1,H2
2265  END IF
2270  IF Ivd=0 AND Jop=0 THEN
2275  PRINT USING "10X,""Inlet temp (Deg C) :"",5(DDD.DD,2X)";Ti(*)
2280  PRINT USING "10X,""Outlet temp (Deg C):"",5(DDD.DD,2X)";To(*)
2285  PRINT USING "10X,""Saturation temperature = "",3D.DD,"" (Deg C)""";Tsat
2290  PRINT USING "10X,""Degree of superheat    = "",3D.DD,"" (Deg C)""";Dsup
2295  PRINT USING "10X,""Static pressure        = "",3D.DD,"" (mm Hg)""";Pvap
2300  END IF
2305!
2310! CALCULATE AVERAGE BULK TEMPERATURES
2315!
2320  IF Ivd=0 THEN Nx=4
2325  IF Ivd=1 THEN Nx=0
2330  FOR I=0 TO Nx
2335  Tb(I)=(Ti(I)+To(I))*.5
2340  NEXT I
2345!
2350  IF Mi=1 OR (Mi=2 AND Nrun<6) THEN As1=0.
2355  IF Mi=2 AND Nrun>5 THEN S1=As1
2360  S1=As1
2365  FOR J=0 TO Nx
2370  IF J=0 THEN Cwf=Fm1
2375  IF J=1 THEN Cwf=Fm2
2380  Mf=Mfi(J)+Mfs(J)*Cwf
2385  Tx=Tb(J)
2390  Vw(J)=Mf/(FNRhow(Tx)*Ai)
2395!
2400! CALCULATE INSIDE AND OUTSIDE COEFFICIENTS
2405!
2410  Rew=FNRhow(Tx)*Vw(J)*Di/FNMuw(Tx)
2415  Cf=1.
2420  Q=Mf*FNCpw(Tx)*(To(J)-Ti(J))
2425  IF Nrun=1 AND J=0 THEN Q1=Q
2430  Qp=Q/(PI*Do*L)
2435  IF (Mi=1 OR (Mi=2 AND Nrun<6)) AND J=0 THEN
2440  Tfilm=Tsat
2445  Kf=FNKw(Tfilm)
2450  Rhof=FNRhow(Tfilm)
2455  Hfg=FNHfg(Tsat)*1000
2460  Muf=FNMuw(Tfilm)
2465  Hnu=.651*Kf*(Rhof^2*Hfg*9.799/(Muf*Do*Qp))^.3333
2470  Tfilmc=Tsat-Qp/Hnu*.5
2475  IF ABS((Tfilmc-Tfilm)/Tfilmc)>.01 THEN
2480  Tfilm=Tfilmc
2485  GOTO 2445
2490  END IF
2495  IF Ivd=0 AND Jop=0 THEN
2500  PRINT USING "10X,""Nusselt coefficient for first tube = "",5D.D,"" (W/m^2.
K)""";Hnu
2505  END IF
```

```
2510 END IF
2515 IF J=0 AND Ivd=0 AND Jop=0 THEN
2520 IF Mi=1 AND Nrun=1 THEN Ho1=0.
2525 PRINT "          Tube     Vw    Heat flux    Cond coef     R1      R2
 RR"
2530 PRINT "            #    (m/s)    (W/m 2)     (W/m 2.K)"
2535 END IF
2540 IF Nrun=1 AND Ivs=1 AND Ivd=0 THEN
2545 Vg=FNVvst(Tsat)
2550 Vv=Mdot*Vg/Af
2555 Dt=(Tsat-Tfilm)*2
2560 Muf=FNMuw(Tfilm)
2565 Hfg=FNHfg(Tsat)*1000
2570 Kf=FNKw(Tfilm)
2575 Rhof=FNRhow(Tfilm)
2580 Retp=Rhof*Vv*Do/Muf
2585 Ff=9.799*Do*Muf*Hfg/(Vv^2*Kf*Dt)
2590 IF Ivd=0 THEN
2595 Nuc=B*Ff^Nvs*Retp^.5
2600 Hoc=Nuc*Kf/Do
2605 Tfilmc=Tsat-Qp/Hoc*.5
2610 IF ABS(Tfilm-Tfilmc)>.1 THEN
2615 Tfilm=Tfilmc
2620 GOTO 2555
2625 END IF
2630 END IF
2635 END IF
2640 Muw=FNMuw(Tx)
2645 Hi=FNKw(Tx)/Di*Ci*Rew^Ex*(FNPrw(Tx))^.3333*Cf
2650 Dt=Qp/Hi*Do/Di
2655 Cfc=(Muw/(FNMuw(Tx+Dt)))^.14
2660 IF ABS((Cf-Cfc)/Cfc)>.01 THEN
2665 Cf=(Cf+Cfc)*.5
2670 GOTO 2645
2675 END IF
2680 Lmtd=(To(J)-Ti(J))/LOG((Tsat-Ti(J))/(Tsat-To(J)))
2685 IF Nrun=1 AND Ivs=1 AND Ivd=0 THEN
2690 Fc(J)=Hoc/Hnu*(Q/Q1)^.3333
2695 Mdot=Mdot-Q/Hfg
2700 END IF
2705 Uo=Qp/Lmtd
2710 Ho(J)=1/(1/Uo-Do/(Di*Hi)-Rw)
2715 IF Ivd=1 THEN
2720 Dt=Qp/Ho(0)
2725 Tfilm=Tsat-Dt/2
2730 Vg=FNVvst(Tsat)
2735 Rhof=FNRhow(Tfilm)
2740 Vv=Mdot*Vg/Af
2745 Muf=FNMuw(Tfilm)
2750 Kf=FNKw(Tfilm)
2755 Hfg=FNHfg(Tsat)*1000
2760 Retp=Rhof*Vv*Do/Muf
2765 Ff=9.799*Do*Muf*Hfg/(Vv^2*Kf*Dt)
2770 Nuc=Ho(0)*Do/Kf
2775 Y=LOG(Nuc/Retp^.5)
2780 F=LOG(Ff)
2785 Sgy=Sgy+Y
2790 Sgf=Sgf+F
2795 Sgyf=Sgyf+Y*F
2800 Sgf2=Sgf2+F^2
2805 END IF
```

```
2810  IF Ivd=0 THEN
2815  IF Ivs=1 THEN Ho(J)=Ho(J)/Fc(J)
2820  Rr=Uo/Ho(J)
2825  S1=S1+Ho(J)
2830  IF Nrun MOD 5=1 THEN
2835  IF Mi=1 OR (Mi=2 AND Nrun=31) THEN Ja=0
2840  IF Mi=2 AND 5<Nrun AND Nrun<30 THEN Ja=Nrun-1
2845  IF Mi=2 AND 35<Nrun THEN Ja=Nrun-1
2850  END IF
2855  IF Mi=1 OR (30<Nrun AND Nrun<36 AND Mi=1) OR Nrun<6 THEN
2860  R1=Ho(J)/Ho(0)
2865  R2=S1/((J+1+Ja)*Ho(0))
2870  ELSE
2875  R1=Ho(J)/Ho1
2880  R2=S1/((J+1+Ja)*Ho1)
2885  END IF
2890!
2895! PRINT RESULTS
2900!
2905  IF Jop=0 THEN
2910  PRINT USING "11X,DD,4X,DD.DD,2X,2(D.5DE,2X),3(Z.4D,2X)";J+1+Ja,Vw(J),Qp,Ho
(J),R1,R2,Rr
2915  IF Im=1 AND J=4 THEN
2920  BEEP
2925  INPUT "OK TO ACCEPT THIS DATA SET (1=Y,0=N)?",Oks
2930  IF Oks<>1 THEN
2935  Nrun=Nrun-1
2940  GOTO 1650
2945  END IF
2950  END IF
2955  END IF
2960!
2965  IF Mi=2 AND Nrun<6 AND J=0 THEN
2970  Ho1=Ho1+Ho(0)/5
2975  END IF
2980  FOR K=0 TO 4
2985  IF K=J THEN S3(K)=S3(K)+R1
2990  IF K=J THEN S4(K)=S4(K)+R2
2995  NEXT K
3000  END IF
3005  NEXT J
3010  IF Ivd=0 THEN
3015  IF Nrun MOD 5=0 THEN
3020  FOR K=0 TO 4
3025  R3(K)=S3(K)/5
3030  R4(K)=S4(K)/5
3035  S3(K)=0.
3040  S4(K)=0.
3045  NEXT K
3050  IF Mi=2 AND Nrun MOD 5=0 AND Nrun<>30 THEN As1=Nrun*R4(4)*Ho1
3055!
3060! PRINT AVERAGE RATIOS
3065!
3070  IF Jop=0 OR (Jop=1 AND Nrun<6) THEN
3075  PRINT
3080  PRINT "            Tube #     R3         R4"
3085  END IF
3090  FOR J=1 TO 5
3095  PRINT USING "12X,DD,2(4X,Z.4D)";J+Ja,R3(J-1),R4(J-1)
3100  OUTPUT @File3;J+Ja,R3(J-1),R4(J-1)
3105  NEXT J
```

```
3110  END IF
3115  IF Nrun MOD 5=0 AND Mi=2 AND Nrun<>30 AND Im=1 THEN
3120  BEEP
3125  PRINT USING "10X,""Set porous-tube flowmeter reading to "",3D.D,"" PERCENT
"""";Set
3130  END IF
3135  END IF
3140  IF Ivd=1 THEN
3145  Ey=EXP(Y)
3150  PRINT USING "12X,DD,5X,Z.DD,2X,Z.3DE,2X,3D.DD,2X,2(Z.3D,2X)";Nrun,Vv,Retp,
Nuc,Ey,Ff
3155  IF Im=1 THEN
3160  BEEP
3165  INPUT "OK TO ACCEPT THIS DATA SET (1=Y,0=N)?",Oks
3170  IF Oks<>1 THEN
3175  Nrun=Nrun-1
3180  GOTO 1605
3185  END IF
3190  END IF
3195  OUTPUT @File3;Ff,Ey
3200  END IF
3205!
3210  IF Nrun MOD 5=1 AND Mi=2 AND Nrun>5 AND Im=1 THEN
3215  OUTPUT @File1;Set
3220  Mpt=-8.361613+10.076742*Set
3225  END IF
3230  IF Im=1 THEN
3235  OUTPUT @File1;Ti(*),To(*),Tsa,Tcon,Tv,Pvap,Tsat,Dsup,Fm1,Fm2
3240  OUTPUT @File1;H1,H2
3245  BEEP
3250  INPUT "WILL THERE BE ANOTHER RUN (1=Y,0=N)?",Go_on
3255  IF Go_on=1 THEN
3260  IF Ivd=0 THEN 1650
3265  IF Ivd=1 THEN 1605
3270  END IF
3275  ELSE
3280  IF Mi=2 AND Nrun<30 THEN
3285  IF Ivd=0 THEN 1650
3290  IF Ivd=1 THEN 1605
3295  END IF
3300  IF Mi=1 AND Nrun<10 THEN
3305  IF Ivd=0 THEN 1650
3310  IF Ivd=1 THEN 1605
3315  END IF
3320  END IF
3325  IF Im=1 THEN PRINT USING "10X,DD,"" Data runs were stored in file "",10A";
Nrun,Newdata$
3330  PRINT
3335  PRINT USING "10X,""Plot data are stored in file "",14A";File_out$
3340  IF Ivd=1 THEN
3345  Nvs=(Nrun*Sgyf-Sgy*Sgf)/(Nrun*Sgf2-Sgf 2)
3350  B=EXP((Sgy-Nvs*Sgf)/Nrun)
3355  PRINT
3360  PRINT USING "10X,""Vapor-Shear Correlation:"""
3365  PRINT USING "12X,""B     = "",Z.3D";B
3370  PRINT USING "12X,""n     = "",Z.3D";Nvs
3375  END IF
3380  ASSIGN @File1 TO *
3385  ASSIGN @File2 TO *
3390  ASSIGN @File3 TO *
3395  SUBEND
```

AD-A158 895 THE EFFECT OF CONDENSATE INUNDATION ON STEAM CONDENSATION HEAT TRANSFER IN A TUBE BUNDLE(U) NAVAL POSTGRADUATE SCHOOL MONTEREY CA S K BROWER JUN 85 2/2

UNCLASSIFIED F/G 20/13 NL

END

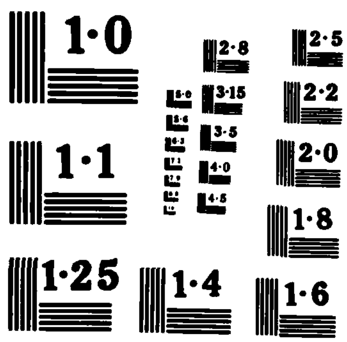

NATIONAL BUREAU OF STANDARDS
MICROCOPY RESOLUTION TEST CHART

```
3400!
3405! THIS SUROUTINE CONVERTES THERMOCOUPLE VOLTAGE INTO TEMPERATURE
3410!
3415  SUB Tvsv(T)
3420  COM /C1/ C(7)
3425  Sum=0.
3430  FOR I=0 TO 7
3435  Sum=Sum+C(I)*T^I
3440  NEXT I
3445  T=Sum
3450  SUBEND
3455!
3460! THIS FUNCTION CALCULATES PRANDTL NUMBER OF WATER IN THE
3465! RANGE 15 TO 45 DEG C
3470!
3475  DEF FNPrw(T)
3480  Y=10^(1.09976605-T*(1.3749326E-2-T*(3.968875E-5-3.45026E-7*T)))
3485  RETURN Y
3490  FNEND
3495!
3500! THIS FUNCTION CALCULATES THERMAL CONDUCTIVITY OF WATER
3505! IN THE RANGE OF 15 TO 105 DEG C
3510!
3515  DEF FNKw(T)
3520  Y=.5625894+T*(2.2964546E-3-T*(1.509766E-5-4.0581652E-8*T))
3525  RETURN Y
3530  FNEND
3535!
3540! THIS FUNCTION CALCULATES SPECIFIC HEAT OF WATER
3545! IN THE RANGE 15 TO 45 DEG C
3550!
3555  DEF FNCpw(T)
3560  Y=(4.21120858-T*(2.26826E-3-T*(4.42361E-5+2.71428E-7*T)))*1000
3565  RETURN Y
3570  FNEND
3575!
3580! THIS FUNCTION CALCULATES DENSITY OF WATER IN THE
3585! RANGE 15 TO 105 DEG C
3590!
3595  DEF FNRhow(T)
3600  Ro=999.52946+T*(.01269-T*(5.482513E-3-T*1.234147E-5))
3605  RETURN Ro
3610  FNEND
3615!
3620! THIS FUNCTION APPLIES CORRECTIONS TO THERMOCOUPLE READINGS
3625!
3630  DEF FNTemp(T,I)
3635  DIM A(14),B(14)
3640  DATA 0.640533,0.573054,0.593101,0.57298,0.56228,0.567384,0.569577
3645  DATA 0.553951,0.552008,0.566955,0.520998,0.522661,0.531008,0.560788,0.5524
05
3650  DATA 11.8744,8.63163,9.39412,8.570246,8.299436,8.36677,8.04507,7.459766
3655  DATA 7.498928,7.9408,5.87072,5.391556,6.13399,6.48586,6.326224
3660  READ A(*),B(*)
3665  IF I<15 THEN
3670  T=T-(A(I)-B(I)*.001*T)
3675  ELSE
3680  T=T-.5
3685  END IF
3690  RETURN T
3695  FNEND
```

```
3700!
3705! THIS FUNCTION COMPUTES THE SPECIFIC VOLUME OF STEAM
3710!
3715  DEF FNVvst(Tt)
3720  P=FNPvst(Tt)
3725  T=Tt+273.15
3730  X=1500/T
3735  F1=1/(1+T*1.E-4)
3740  F2=(1-EXP(-X))^2.5*EXP(X)/X^.5
3745  B=.0015*F1-.000942*F2-.0004882*X
3750  K=2*P/(461.52*T)
3755  V=(1+(1+2*B*K)^.5)/K
3760  RETURN V
3765  FNEND
3770!
3775! THIS FUNCTION CONVERTS THE VOLTAGE READING OF THE PRESSURE
3780! TRANSDUCER INTO PRESSURE IN MM HG
3785!
3790  DEF FNPvsv(V)
3795  Y=1.1103462+163.36413*V
3800  RETURN Y
3805  FNEND
3810!
3815! THIS FUNCTION CALCULATES THE SATURATION TEMPERATURE OF STEAM AS A FUNCTION
3820! OF PRESSURE
3825!
3830  DEF FNTvsp(P)
3835  Tu=110
3840  Tl=80
3845  Ta=(Tu+Tl)*.5
3850  Pc=FNPvst(Ta)
3855  IF ABS((P-Pc)/P)>.0001 THEN
3860  IF Pc<P THEN Tl=Ta
3865  IF Pc>P THEN Tu=Ta
3870  GOTO 3845
3875  END IF
3880  RETURN Ta
3885  FNEND
3890!
3895! THIS FUNCTION COMPUTES THE VISCOSITY OF WATER
3900!
3905  DEF FNMuw(T)
3910  A=247.8/(T+133.15)
3915  Mu=2.4E-5*10^A
3920  RETURN Mu
3925  FNEND
3930!
3935! THIS FUNCTION COMPUTES THE LATENT HEAT OF VAPORIZATION
3940!
3945  DEF FNHfg(T)
3950  Hfg=2497.7389-T*(2.2074+T*(1.7079E-3-2.8593E-6*T))
3955  RETURN Hfg
3960  FNEND
3965!
3970! THIS FUNCTION COMPUTES THE SATURATION PRESSURE
3975!
3980  DEF FNPvst(Tsteam)
3985  DIM K(8)
3990  DATA -7.691234564,-26.08023696,-168.1706546,64.23285504,-118.9646225
3995  DATA 4.16711732,20.9750676,1E9,6
```

```
4000  READ K(*)
4005  T=(Tsteam+273.15)/647.3
4010  Sum=0
4015  FOR N=0 TO 4
4020  Sum=Sum+K(N)*(1-T)^(N+1)
4025  NEXT N
4030  Br=Sum/(T*(1+K(5)*(1-T)+K(6)*(1-T)^2))-(1-T)/(K(7)*(1-T)^2+K(8))
4035  Pr=EXP(Br)
4040  P=22120000*Pr
4045  RETURN P
4050  FNEND
4055!
4060! THIS FUNCTION CALCULATES THE STEAM MASS FLOW RATE
4065!
4070  DEF FNMdot(Dp)
4075  Mdot=4.3183E-3+5.6621E-4*Dp
4080  RETURN Mdot
4085  FNEND
```

APPENDIX D

SEIDER-TATE CONSTANT CALCULATION

The following solution procedure used in calculating the Sieder-Tate constant, by using a modified Wilson plot, is presented in this appendix:

1. The overall heat-transfer coefficient is defined as:

$$\frac{1}{U_o} = \frac{1}{h_o} + R_w + \frac{D_o}{D_i\ h_i} \qquad \text{(D.1)}$$

2. The Nusselt number is defined as:

$$Nu = h_i\ D_i\ /\ k_c$$

or

$$Nu = C_i\ Re^{0.8}\ Pr^{1/3}\ (\mu_c/\mu_w)^{0.14} \qquad \text{(D.2)}$$

or

$$Nu = C_i\ \Omega\ ;\ \text{where} \qquad \text{(D.2a)}$$

$$\Omega = Re^{0.8}\ Pr^{1/3}\ (\mu_c/\mu_w)^{0.14}$$

3. By using the Nusselt equation:

$$h_o = 0.725\left[\frac{k_f^{\ 3}\ \rho_f^{\ 2}\ h_{fg}\ g}{\mu_f\ D_o\ (T_{sat}-T_w)}\right]^{1/4} \qquad \text{(D.3)}$$

and

$$q = h_o\ (T_{sat}-T_w) \qquad \text{(D.4)}$$

and upon combining equations (D.3) and (D.4)

$$h_o = 0.651\left[\frac{k_f^{\ 3}\ \rho_f^{\ 2}\ h_{fg}\ g}{\mu_f\ D_o\ q}\right]^{1/3} \qquad \text{(D.5)}$$

or $$h_o = 0.651\ \nu^{1/3} \text{ ; where} \tag{D.5a}$$

$$\nu = \frac{k_f^{\,3}\ \rho_f^{\,2}\ h_{fg}\ g}{\mu_f\ D_o\ q}$$

4. Substituting equations (D.2a) and (D.5a) into equation (D.1), and rearranging gives:

$$\left(\frac{1}{U_o} - R_w\right) \nu^{1/3} = \frac{1}{C_i} \frac{D_o\ \nu^{1/3}}{k_c\ \Omega} + \frac{1}{0.0651} \tag{D.6}$$

or $Z = m\ W + 1/0.0651$; where

$$Z = \left(\frac{1}{U_o} - R_w\right) \nu^{1/3} ,$$

$$m = 1\ /\ C_i \quad \text{and}$$

$$W = D_o\ \nu^{1/3}\ /\ k_c\ \Omega$$

5. By plotting Z vs. W and computing the slope of the least-squares-fit line, and then taking the reciprocal of this slope, the resulting value is the Sieder-Tate constant.

NOTE: T_w and T_f must be determined iteratively, as described in Chapter IV, section E.

LIST OF REFERENCES

1. Search, H.T., A Feasibility Study of Heat Transfer Improvements in Marine Steam Condensers, MSME Thesis, Naval Postgraduate School, Monterey, CA, January 1977.

2. Beck, A.C., A Test Facility to Measure Heat Transfer Performance of Advanced Condenser Tubes, MSME Thesis, Naval Postgraduate School, Monterey, CA, March 1978.

3. Pence, D.T., An Experimental Study of Steam Condensation on a Single Horizontal Tube, MSME Thesis, Naval Postgraduate School, Monterey, CA, March 1978.

4. Reilly, D.J., An Experimental Investigation on Enhanced Heat Transfer of Horizontal Condenser Tubes, MSME Thesis, Naval Postgraduate School, Monterey, CA, March 1978.

5. Fenner, J.H., An Experimental Comparison of Enhanced Heat Transfer Condenser Tubing, MSME Thesis, Naval Postgraduate School, Monterey, CA, March 1978.

6. Ciftci, H., An Experimental Study of Filmwise Condensation on Horizontal Enhanced Condenser Tubing, MSME Thesis, Naval Postgraduate School, Monterey, CA, December 1979.

7. Marto, P.J., Reilly, D.J., Fenner, J.H., "An Experimental Comparison of Enhanced Heat Transfer Tubing," Advances in Enhanced Heat Transfer, Proceedings of the 18th National Heat Transfer Conference, American Society of Mechanical Engineers, New York, NY, 1979.

8. Webb, R.L., "The Use of Enhanced Surface Geometries in Condensers: An Overview," Power Condenser Heat Transfer Technology, Marto, P.J. and Nunn, R.H. (Eds.), Hemisphere Publishing Corp., New York, 1980, pp. 287-318.

9. Thomas, A., Lorenz, J.J., Hillis, D.A., Young, D.T. and Sather, N.F., "Performance Tests of the 1 MWT Shell and Tube Exchanger for OTEC," Proceedings of the 6th OTEC Conference, Paper 3c, June 1979.

10. Nusselt, W., "Die Oberflachen-Kondensation des Wasserdampfes," VDI Zeitung, Vol. 60, 1916, pp. 541-546 and pp. 569-575.

11. Cunningham, J., "The Effect of Noncondensable Gases on Enhanced Surface Condensation," Power Condenser Heat Transfer Technology, Marto, P.J. and Nunn, R.H. (Eds.), Hemisphere Publishing Corp., New York, 1980, pp. 353-365.

12. Kanakis, G.D., The Effect of Condensate Inundation on Steam Condensation Heat Transfer to Wire-Wrapped Tubing, MSME Thesis, Naval Postgraduate School, Monterey, CA, June 1983.

13. Tanasawa, I., "Dropwise Condensation: The Way to Practical Applications," Proceedings of the Sixth International Heat Transfer Conference, Vol. 6, Toronto, 1978, pp. 393-405.

14. Brown, A.R. and Thomas, M.A., "Filmwise and Dropwise Condensation of Steam at Low Pressure," Proceedings of the Third International Heat Journal Conference, Vol. 2, Chicao, 1966, pp. 300-305.

15. Holden, K.N., An Evaluation of 'Permanent' Organic Coatings for the Promotion of Dropwise Condensation of Steam, ME Thesis, Naval Postgraduate School, Monterey, CA, March 1984.

16. Nobbs, D.W., The Effect of Downward Vapour Velocity and Inundation on the Condensate Rates on Horizontal Tube Banks, Ph.D. Thesis, University of Bristol, England, April 1975.

17. Jakob, M., Heat Transfer, Vol. 1, J. Wiley and Sons, Inc., 1948, pp. 667-673.

18. Kern, D.Q., "Mathematical Development of Loading in Horizontal Condensers," AIChE Journal, Vol. 4, 1958, pp. 157-160.

19. Eissenberg, D.M., An Investigation of the Variables Affecting Steam Condensation on the Outside of a Horizontal Tube Bundle, Ph.D. Thesis, University of Tennessee, Knoxville, TN, December 1972.

20. Berman, L.D., "Heat Transfer with Steam Condensation on a Bundle of Horizontal Tubes," Thermal Engineering, Vol. 28, 1981, pp. 218-224.

21. Marto, P.J. and Wanniarachchi, A.S., "The Use of Wire-Wrapped Tubing to Enhance Steam Condensation in Tube Bundles," Submitted for Presentation at the ASME Winter Annual Meeting, New Orleans, December 1984.

22. Chisholm, D., "Modern Developments in Marine Condensers: Noncondensable Gases: An Overview," Power Condenser Heat Transfer Technology, Marto, P.J. and Nunn, R.H. (Eds.), Hemisphere Publishing Corp., New York, 1981, pp. 95-142.

23. Webb, R.L. and Wanniarachchi, A.S., "The Effect of Non-condensable Gases in Water Chiller Condenser--Literature Survey and Theoretical Predictions," ASHRAE Transactions, Vol. 86, Part 1, 1980, pp. 142-159.

24. Berman, L.D. and Tumanov, Y.A., "Investigation of Heat Transfer in the Condensation of Moving Steam on a Horizontal Tube," Teploenergitika, Vol. 9, 1962, pp. 77-83.

25. Shekriladze, I.G. and Gomelauri, V.I., "Theoretical Study of Laminar Film Condensation of Flowing Vapor," International Journal of Heat and Mass Transfer, Vol. 9, 1966, pp. 581-591.

26. Fujii, T., Uehara, H. and Kurata, C., "Laminar Filmwise Condensation of Flowing Vapor on a Horizontal Cylinder," International Journal of Heat and Mass Transfer, Vol. 15, 1972, pp. 235-246.

27. Marto, P.J., "Heat Transfer and Two-Phase Flow During Shell-Side Condensation," ASME/JSME Thermal Engineering Joint Conference Proceedings, Vol. 2, pp. 567-591.

28. Fujii, T., "Vapor Shear and Condensate Inundation: An Overview," Power Condenser Heat Transfer Technology, Marto, P.J. and Nunn, R.H. (Eds.), Hemisphere Publishing Corp., New York, 1981, pp. 193-223.

29. Morrison, R.H., A Test Condenser to Measure Condensate Inundation Effects in a Tube Bundle, MSME Thesis, Naval Postgraduate School, Monterey, CA, March 1981.

30. Noftz, P.J., Effects of Condensate Inundation and Vapor Velocity on Heat Transfer in a Condenser Tube Bundle, MSME Thesis, Naval Postgraduate School, Monterey, CA, June 1982.

31. Holman, J.P., Heat Transfer, 4th Edition, McGraw-Hill, 1976.

32. Incropera, P.F. and Dewitt, P.D., Fundamentals of Heat Transfer, John Wiley and Sons.

33. Kline, S.J. and McClintock, F.A., Describing Uncertainties in Single-Sample Experiments, Mechanical Engineering, Vol. 74, January 1953, pp. 3-8.

INITIAL DISTRIBUTION LIST

		No. Copies
1.	Defense Technical Information Center Cameron Station Alexandria, Virginia 22304-6145	2
2.	Library, Code 0142 Naval Postgraduate School Monterey, California 93943-5100	2
3.	Department Chairman, Code 69 Department of Mechanical Engineering Naval Postgraduate School Monterey, California 93943-5100	1
4.	Professor P.J. Marto, Code 69Mx Department of Mechanical Engineering Naval Postgraduate School Monterey, California 93943-5100	5
5.	Dr. A.S. Wanniarachchi, Code 69Wa Department of Mechanical Engineering Naval Postgraduate School Monterey, California 93943-5100	1
6.	Lt S.K. Brower 1619 Morong Road Bremerton, Washington 98314	1

END

FILMED

10-85

DTIC